Int. J. Electrochem. Sci., 8 **(2013)** 10396 - 10423

International Journal of
ELECTROCHEMICAL
SCIENCE
www.electrochemsci.org

Theoretical Study Of The Structural, Electronic Structure, Fermi Surface, Electronic Charge Density and Optical Properties of the of $LnVO_4$ (Ln= Sm, Eu, Gd and Dy)

A. H. Reshak[1,2], *Sikander Azam*[1,*]

[1] Institute of complex systems, FFPW, CENAKVA, University of South Bohemia in CB, Nove Hrady 37333, Czech Republic
[2] Center of Excellence Geopolymer and Green Technology, School of Material Engineering, University Malaysia Perlis, 01007 Kangar, Perlis, Malaysia
[*]E-mail: sikander.physicst@gmail.com

Received: 18 May 2013 / *Accepted:* 7 July 2013 / *Published:* 1 August 2013

We present first-principles calculations of the electronic structure, Fermi surface, electronic charge density and optical properties of $LnVO_4$ (Ln= Sm, Eu, Gd and Dy) based on density-functional theory using the local density approximation (LDA), generalized-gradient approximation (GGA) and the Engel Vosko GGA formalism (EV-GGA). The calculated band structure and density of states show that $LnVO_4$ compound is metallic. The total DOS at Fermi level $N(E_F)$ were 1.49, 0.95, 1.93 and 4.69 states/eV unit cell, and the bare electronic specific heat coefficient (γ) are 0.26, 0.16, 0.33 and 0.81 mJ/mol-K^2 for $SmVO_4$, $EuVO_4$, $GdVO_4$ and $DyVO_4$, respectively. The Fermi surface of $EuVO_4$ compound is composed of one band and SmVO4, $GdVO_4$ and $DyVO_4$ composed of two bands crossing along the $\Gamma-A$ direction of Brillion zone. The bonding features are analyzed by using the electronic charge density contour in the (1 0 1) crystallographic plane. We found that Ln-O and V-O atoms forms a strong covalent. For further insight information about the electronic structure, the optical properties are derived and analyzed.

Keywords: FPLAPW calculations; Electronic structure; Fermi surface; Charge density; Optical properties; DFT:

1. INTRODUCTION

Despite of their technological importance, which covers a number of applications comprising their use as thermo phosphors, cathodoluminescent materials and scinlillators, until in recent times there has been a drought of high precision structural information for arthovanadate compounds of the

form $LnVO_4$. This situation was cured, at least in fraction, by the fresh report by Chakounmkos et al. [I] of the bursting profile Rietveld structural scrutiny of neutron powder-diffraction data for the zircon-structure $LnVO_4$ compounds with Ln = Sc, Cc, Y, Pr, Nd, Tb, Yb, Er, He, Tin and Lu. Preceding to this investigation, high-precision X-ray diffraction single-crystal structure results were only existing for $CeVO_4$ [2] and $NdVO_4$,[3] whereas lower precision refinements, centered on neutron powder diffraction data, had been accounted for $TbVO_4$, $DyVO_4$, $ErVO_4$, $HoVO_4$ and $YbVO_4$ [4-6].

Whereas the full-profile Rietveld assessments of Chakoulllakos et al. [I] granted accurate crystallographic data for numerous of the rare-earth orthovanadate compounds (plus $ScVO_4$ and YVO_4), neutron-powder diffraction data could not be attained for the lanthanide compounds $EuVO_4$, $SmVO_4$, $EuVO_4$and $GdVO_4$, due to their soaring cross sections for neutron absorption.

Neither experimental nor theoretical details regarding the electronic structure, Fermi surface, electronic charge density and optical properties are available in the literature. The reasons mentioned above motivate us to perform these calculations, using the full potential linear augmented plane wave (FP-LAPW) method in order to provide reference data for the experimentalists and to complete existing theoretical works on this material.

The rest of the paper has been divided in three parts. In Section 2, we briefly describe the computational techniques used in this study. The most relevant results obtained for the electronic structure, Fermi surface, electronic charge density and optical properties for $EuVO_4$, $SmVO_4$, $EuVO_4$ and $GdVO_4$ compounds are presented and discussed in Section 3. Finally, in Section 4 we summarize the main conclusions of our work.

2. CALCULATION METHODOLOGY

The crystal structure of $EuVO_4$, $SmVO_4$, $EuVO_4$ and $GdVO_4$ are shown in Fig.1. The scrutinize compounds have the tetragonal symmetry with space group I41/*amd* (No. 141). The lattice constant for $EuVO_4$ are a=7.2647(9) Å and c= 6.384(1) Å, for $SmVO_4$ are a=7.2358(7) Å and c= 6.362(1) Å, for $EuVO_4$ are a=7.2122(7) Å and c=6.346(2) Å and for $GdVO_4$ are a=7,1429(8) Å and c=6.300(2) Å. The atomic position in sequence for $EuVO_4$, $SmVO_4$, $EuVO_4$ and $GdVO_4$ are given in Table 1.

Table 1. Atomic positions of the $LnVO_4$ compound.

Atoms	x	y	z
Ln = Sm	0000	0.7500	0.1250
V	0000	0.2500	0.3750
O	0.4316(3)	0000	0.2045(4)
Ln= Eu	0000	0.7500	0.1250
V	0000	0.2500	0.3750
O	0.4318(4)	0000	0.2036(6)
Ln= Gd	0000	0.7500	0.1250
V	0000	0.2500	0.3750
O	0.4323(5)	0000	0.2028(7)
Ln= Dy	0000	0.7500	0.1250

V	0000	0.2500	0.3750
O	0.4340(7)	0000	0.2016(6)

We have executed the calculations using the full-potential linear augmented plane wave [FPLAPW] as incorporated in WIEN2K code [7]. This is an implementation of the density functional theory (DFT) [8,9] with different possible approximations for the exchange correlation (XC) potentials. The XC potential were the local density approximation (LDA) of Ceperley–Alderas parameterized by Perdew–Zunger [10], generalized gradient approximation (GGA) of Perdew–Burke–Ernzerhof (PBE) [11], which is based on exchange-correlation energy optimization to calculate the total energy. Also we have used the Engel–Vosko GGA formalism (EVGGA) [12], which optimizes the corresponding potential for band structure calculations. In order to achieve energy eigenvalues convergence, the wave functions in the interstitial region were expanded in plane waves with a cut-off $K_{max} = 7/RMT$, where RMT denotes the smallest atomic muffin-tin sphere radius and Kmax gives the magnitude of the largest K vector in the plane wave expansion. The RMT were taken to be 2.24, 2.23, 2.22 and 2.14 atomic units (a.u.) for Sm, Eu, Gd and Dy respectively and for V and O were 1.62 and 1.43 a.u. A mesh of 2000 **k** points was used in the irreducible Brillion zone integration. In the self consistent field for electronic structure, Fermi surface and optical properties convergence was checked through self consistency. The valence wave functions inside the muffin-tin spheres are expanded up to $l_{max} = 10$, while the charge density was Fourier expanded up to $G_{max} = 12$ (a.u.)$^{-1}$.

3. RESULTS AND DISCUSSION

3.1. Electronic structure

Fig. 2 shows the calculated energy band structure of $LnVO_4$ compounds at equilibrium lattice parameters along the high symmetry directions in the Brillion zone. The valence and conduction bands overlap considerably at the Fermi level as a result these would exhibit metallic properties. More understanding can be achieved from the total and partial density of states (TDOS and PDOS) which are also depicted for the investigated compounds in Fig. 4 and 5. We displayed the calculated results by the EVGGA approximations. With the reason that this approximation gives better band splitting as well optical transition as is clear from the Fig. 4 and 5, that when we replace Sm by Eu and Gd so the peaks shift towards the lower energies and when we replace Gd by Dy again the peaks shifts towards the higher energies.

The peaks between -6.0 eV and -2.0 eV are due to Ln-s/p, V-s/p and O-p states with minimum contribution of O-s states. While the peaks around the Fermi level are due to Ln-f with small contribution of Ln-s/p. The peaks situated between 2.0 eV and 5.0 eV are due to the contribution of V-p/d states with small contribution of O-s state and the peaks from 6.0 eV to 15.0 eV are due to Ln-d and O-s states with small contribution of V-s/p states. There exists a strong hybridization between V-s and V-p in the energy range -6.0 eV and -3.0 eV. Whereas there is strong hybridization around the Fermi level between V-s, V-p and O-s states and also at 2.0 eV there is also a strong hybridization between Ln-d and O-p states.

At the Fermi level E_F, the values of TDOS (EVGGA) for $SmVO_4$, $EuVO_4$, $GdVO_4$ and $DyVO_4$, were 1.49, 0.95, 1.93 and 4.69 states/eV unit cell, respectively. Hence one may to conclude that $DyVO_4$ is more conducting than $SmVO_4$, $EuVO_4$, and $GdVO_4$.

The electronic specific heat coefficient (γ), which is a function of the density of states, can be calculated using the expression $\gamma = \frac{1}{3}\pi^2 \mathrm{N}(\mathrm{E}_F) K_\beta^2$, where $N(E_F)$ is the DOS at the Fermi energy E_F and k_B is the Boltzmann constant. The calculated density of states at the Fermi energy $N(E_F)$ enables us to calculate the bare electronic specific heat coefficient, which is 0.26, 0.16, 0.33 and 0.81 mJ/mol-K^2 for $SmVO_4$, $EuVO_4$, $GdVO_4$ and $DyVO_4$, respectively.

Electron charge density denotes the nature of the bond character. In order to predict the chemical bonding and also the charge transfer in $SmVO_4$, $EuVO_4$, $GdVO_4$ and $DyVO_4$ compounds, the charge-density behaviors in 2D are calculated in the (1 0 1) plane and displayed in Figs 6. The result shows that the substitution of the Sm by Eu, Gd and Dy leads to redistribution of electron charge density i.e. the bond distances increase. As an atom is interchanged by the others the VSCC (valence shell charge carrier) properties changes (Badar et. al). By investigating the influence of replacing Sm by Eu, Gd and Dy in $SmVO_4$, $EuVO_4$, $GdVO_4$ and $DyVO_4$ compounds, it has been found that the charge density around 'Sm' and 'Eu' is greater than both of Gd and Dy atoms. From the calculated electron density it is clear that Ln and O, and also V and O atoms forms a strong covalent bond.

3.2. Fermi surface

It is well established that electronic states crossing the Fermi level are primarily responsible for the Fermi surface (FS) structure and always considered as a key quantity to understand the electronic structure of any metallic material. The conventional way to find out the Fermi surface is to measure energy distribution curves (EDC) for distinct k-points of the Brilliouin zone and to ascertain the k-locations where bands traverse the Fermi energy. The electrons adjacent to the Fermi level are responsible for conductivity, the electronic structure of any metallic material is understandable from the Fermi surface (FS). Fermi surfaces can also be inspected by using de Haas van Alphen (dHvA) experiments, the exact determination of the shape of the FS depends on models using easy geometries to define the magnetic field angle dependency of the measured frequencies, but the accurate shape of the FS can of course be much further complex. Therefore we figured the FS of $SmVO_4$, $EuVO_4$, $GdVO_4$ and $DyVO_4$ using the FPLAPW method outlined above. The results are shown in Fig 7.

The Fermi surface of $EuVO_4$ compound is composed of one band while SmVO4, $GdVO_4$ and $DyVO_4$ composed of two bands crossing along the Γ−A direction of Brillion zone. The $SmVO_4$, $EuVO_4$, $GdVO_4$ and $DyVO_4$ Fermi surface consist of a set of holes and electronic sheets, where the empty areas contain holes and shaded areas electrons.

In the four compounds a considerable differences there exists in the FS topology, due to changes in inter- atomic distances, bonding angles and as well as to the degree of band filling (Fig. 7). In the Fermi surface the color changes occur due to the change in electron velocity. The red and violet color shows fast and the slow velocity of electrons while the remaining colors have the intermediate

velocity of electron. The structure of the four compounds are considerably the same but the changes occur in the color which resulting the change in velocity of electron.

3.3. Optical Properties

Study the optical properties of solids has been an interesting research topic in basic research as well as for industrial applications. In basic research the origin and nature of different excitation processes are of fundamental interest and in the industrial applications can make use of them in many optoelectronic devices. Therefore optical properties bring together experiment and theory. The calculation of $\varepsilon_2(\omega)$ requires energy eigen-values and electron wave functions. These are natural outputs of a band structure calculation. The interband transitions of the dielectric function can be split into direct and indirect transitions. We overlook the indirect inter-band transitions involving scattering of phonons that are expected to give a small contribution to $\varepsilon(\omega)$ [13]. To compute the direct inter-band contributions to the imaginary part of the dielectric function $\varepsilon_2(\omega)$, it is essential to operate summation up all likely transitions from the occupied to the unoccupied states. These compounds are crystallized in the I41/*amd* (#= 141) space group. This symmetry group has two dominant independent components of the dielectric tensor. The corresponding dielectric functions are $\varepsilon_2^{xx}(\omega)$ and $\varepsilon_2^{zz}(\omega)$ corresponding to the applied electric field (corresponding to light polarization) parallel and perpendicular to the crystallographic c-axis. Taking the appropriate transition matrix elements into account, we calculated the imaginary part of the dielectric functions $\varepsilon_2(\omega)$ using the expressions given in the Refs. [14–16]:

$$\varepsilon_2{}^{xx}(\omega) = \frac{\S}{m\omega^2}\int_{BZ}\sum_{nn'}\frac{\left[\left|P^x{}_{nm'}\left(k\right)\right|^2 + \left|P^y{}_{nm'}\left(k\right)\right|^2\right] dS_k}{\nabla\omega_{nm'}(k)} \quad \ldots\ldots. (1)$$

$$\varepsilon_2{}^{zz}(\omega) = \frac{12}{m\omega^2}\int_{BZ}\sum_{nn'}\frac{\left|P^z{}_{nm'}\left(k\right)\right|^2 dS_k}{\nabla\omega_{nm'}(k)} \quad \ldots\ldots\ldots (2)$$

The above terms are written in atomic units with e^2 =1/m=2 and ħ=1, where ω is the photon energy. $P^x{}_{nm'}(k)$ and $P^z{}_{nm'}(k)$ are the X and Z component of the dipolar matrix elements between initial $|n'k\rangle$ and final $|n'k\rangle$ states with their eigenvalues $E_n(k)$ and $E'_n(k)$ respectively. $\omega_{n'n}(k)$ is the energy difference, where $\omega_{n'n}(k)$= $E_n(k)$ - $E'_n(k)$ and S_k is a constant energy surface with $S_k = \{k;\omega_{nn'}(k)=\omega\}$. The integration is done over the first irreducible Brillion zone (IBZ).

Since the investigated compounds have metallic nature thus we have to include the intra band transitions (Drude term). Therefore both of the intra-band and inter-band transitions are contribute:

$$\varepsilon_2(\omega) = \varepsilon_{2inter}(\omega) + \varepsilon_{2intra}(\omega)\ldots\ldots\ldots (3)$$

where

$$\varepsilon^{xx}{}_{2intra}(\omega) = \frac{\omega^{xx}{}_p\tau}{\omega\left(1+\omega^2\tau^2\right)}\ldots\ldots (4)$$

$$\varepsilon^{zz}{}_{2intra}(\omega) = \frac{\omega^{zz}{}_p\tau}{\omega\left(1+\omega^2\tau^2\right)}\ldots\ldots\ldots (5)$$

where τ and ω_p [51] is mean free time and mean frequency amongst the collisions.

$$\omega_p{}^2 = \frac{8\pi}{3}\sum_{kn} \vartheta^2{}_{kn}\delta(\varepsilon_{kn}) \ldots\ldots\ldots (6)$$

As ε_{kn} is $\mathrm{E}_n(k) - \mathrm{E}_F$ and ϑ_{kn} is the velocity of electron.

The calculated valves of $\hbar\omega_p$ corresponding to two polarizations parallel and perpendicular to c-axis are given in Table. 2.

Table 2. The calculated plasma energy in eV of the $LnVO_4$ compound.

Compounds	$\hbar\omega_p^{xx}$	$\hbar\omega_p^{zz}$
$SmVO_4$	0.40	8.21
$EuVO_4$	0.68	8.27
$GdVO_4$	0.42	8.32
$DyVO_4$	0.65	0.73

For the metallic materials there are two contributions to $\varepsilon(\omega)$, namely intra-band and inter-band transitions. Fig. 8, illustrates the variation of the imaginary part of the frequency dependent electronic dielectric function $\varepsilon_2(\omega)$. The calculated imaginary part $\varepsilon_2(\omega)$ can be used to describe the transitions between the occupied and unoccupied bands. It can be seen from $\varepsilon_2(\omega)$ spectra that the spectral features of the optical properties for the investigated compounds are looking different that is ascribed to the fact that the band structures of these compounds acquire different dispersion as a consequence the allowed optical transition are occurs between different states, resulting in different dispersion of the spectral features of the optical susceptibilities suggesting that moving through the periodic table from left to right replacing the element Sm by Eu, Gd and Dy, show there is a considerable change in the dispersion of the spectral features of the optical properties. We should emphasize that there is a considerable anisotropy between $\varepsilon_2^{xx}(\omega)$ and $\varepsilon_2^{zz}(\omega)$ components. The peaks in the optical response are caused by the allowed electric-dipole transitions between the valence and conduction bands. In order to identify these structures we should consider the magnitude of the optical matrix elements. The observed structures would correspond to those transitions which have large optical matrix dipole transition elements. From the imaginary parts of the dielectric function $\varepsilon_2^{xx}(\omega)$ and $\varepsilon_2^{zz}(\omega)$ the real parts $\varepsilon_1^{xx}(\omega)$ and $\varepsilon_1^{zz}(\omega)$ can be calculated using Kramers–Kronig relations [17]. Our calculated real parts are illustrated in Fig. 9. Again we find a considerable anisotropy between $\varepsilon_1^{xx}(\omega)$ and $\varepsilon_1^{zz}(\omega)$.

4. CONCLUSION

In summary, we calculate the electronic structure, Fermi surface, charge density and optical properties of $EuVO_4$, SmVO4, $EuVO_4$, $GdVO_4$ and $DyVO_4$ compounds by means of DFT within LDA, GGA and EVGGA. The investigated compounds possess metallic nature, the values of DOS at E_F ($N(E_F)$) were 1.49, 0.95, 1.93 and 4.69 states/eV unit cell, and the bare electronic specific heat

coefficient (γ) are 0.26, 0.16, 0.33 and 0.81 mJ/mol-K^2 for $SmVO_4$, $EuVO_4$, $GdVO_4$ and $DyVO_4$, respectively. The Fermi surface of $EuVO_4$ compound is composed of one band while SmVO4, $EuVO_4$, $GdVO_4$ and $DyVO_4$ composed of two bands crossing along the Γ−A direction of Brillion zone. The bonding features are analyzed by using the electronic charge density contour in the (101) crystallographic plane. The bonding features are analyzed by using the electronic charge density contour in the (101) crystallographic plane. We found that Ln-O and V-O atoms forms a strong covalent. There exists a strong hybridization between V-s and V-p in the energy range -6.0 eV and -3.0 eV. Whereas there is strong hybridization around the Fermi level between V-s, V-p and O-s states and also at 2.0 eV there is also a strong hybridization between Ln-d and O-p states. We also present the dielectric function of SmVO4, $EuVO_4$, $GdVO_4$ and $DyVO_4$ and the imaginary part $\varepsilon_2(\omega)$ of the dielectric function is discussed in detail.

AKNOWLEDEGMENT
This work was supported from the project CENAKVA (No. CZ.1.05/2.1.00/01.0024), the grant No. 134/2013/Z/104020 of the Grant Agency of the University of South Bohemia. School of Material Engineering, Malaysia University of Perlis, P.O Box 77, d/a Pejabat Pos Besar, 01007 Kangar, Perlis, Malaysia

Refrences

1. B.C. Chakoumakos, M.M. Abraham and L.A. Boatner, *J. Solid State Chem*., 109 (1994) 197.
2. K.-J. Range, H. Meister and U. Klement, Z. Naturforsch., *Teil B*, 45 (1990) 598.
3. J.A. Baglio and O.J. Sovers, *J. SolidState Chem*., 3 (1971) 458.
4. E. Pattscheke, H. Feuss and G. Will, *Chem. Phys. Leg*., 2 (1968) 47.
5. G. Will and W. Schafer, *J. Phys. C*, 4 (1971) 811.
6. H. Feuss and A. Kallel, *.L Solid State Chem*. 5 (1972) 1.
7. P.Blaha, K. Schwarz, J. Luitz WIEN97, A full potential linearized augmented plane wave package for calculating crystal properties, Karlheinz Schwarz, Techn. Universit at Wien, Austria, 1999.ISBN:3-9501031-0-4.
8. P. Hohenberg, W. Kohn, *Phys. Rev*. 136 (1964) B864.
9. W. Kohn, L. J. Shom, *Phys. Rev*. 140 (1965) A1133.
10. J. P. Perdew, A. Zunger, *Phys. Rev*. B23 (1981) 5048.
11. J. P. Perdew, K. Burke, M. Ernzerhof, *Phys. Rev. Lett*. 77(1996)3865.
12. E. Engel, S. H. Vosko, *Phys. Rev.* B50 (1994)10498.
13. N.V. Smith, Phys. Rev. B 3 (1862) 1971.
14. S. Hufner, R. Claessen, F. Reinert, Th. Straub, V.N. Strocov, P. Steiner, *J. Electron Spectrosc*. Relat. Phenom. 100 (1999) 191; R. Ahuja, S. Auluck, B. Johansson, M.A. Khan, *Phys. Rev. B* 50 (1994) 2128.
15. A.H. Reshak, I.V. Kityk, S. Auluck, *J. Chem. Phys.* 129 (2008) 074706.
16. M.B. Kanoun, S. Goumri-Said, A.H. Reshak, *Comput. Mater. Sci*. 47 (2009) 491.
17. H. Tributsch, *Z. Naturforsch*. 32a (1977) 972.

Figure 1. Unit cell structure for $LnVO_4$ compound.
Figure 2. Calculated Band structures for $LnVO_4$ compound

Figure 3. Calculated combined total density of state for $LnVO_4$ compound (State/eV unit cell)
Figure 4. Calculated total density of state for $LnVO_4$ compound (State/eV unit cell)
Figure 5. Calculated Partial density of state for $LnVO_4$ compound (State/eV unit cell)
Figure 6. Calculated Fermi surface for $LnVO_4$ compound.
Figure 7. Calculated electron charge density for $LnVO_4$ compounds
Figure 8. Calculated imaginary part of dielectric tenser component for $LnVO_4$ compound $(\varepsilon_2(\omega))$
Figure 9. Calculated real part of dielectric tenser component for $LnVO_4$ compound $(\varepsilon_1(\omega))$

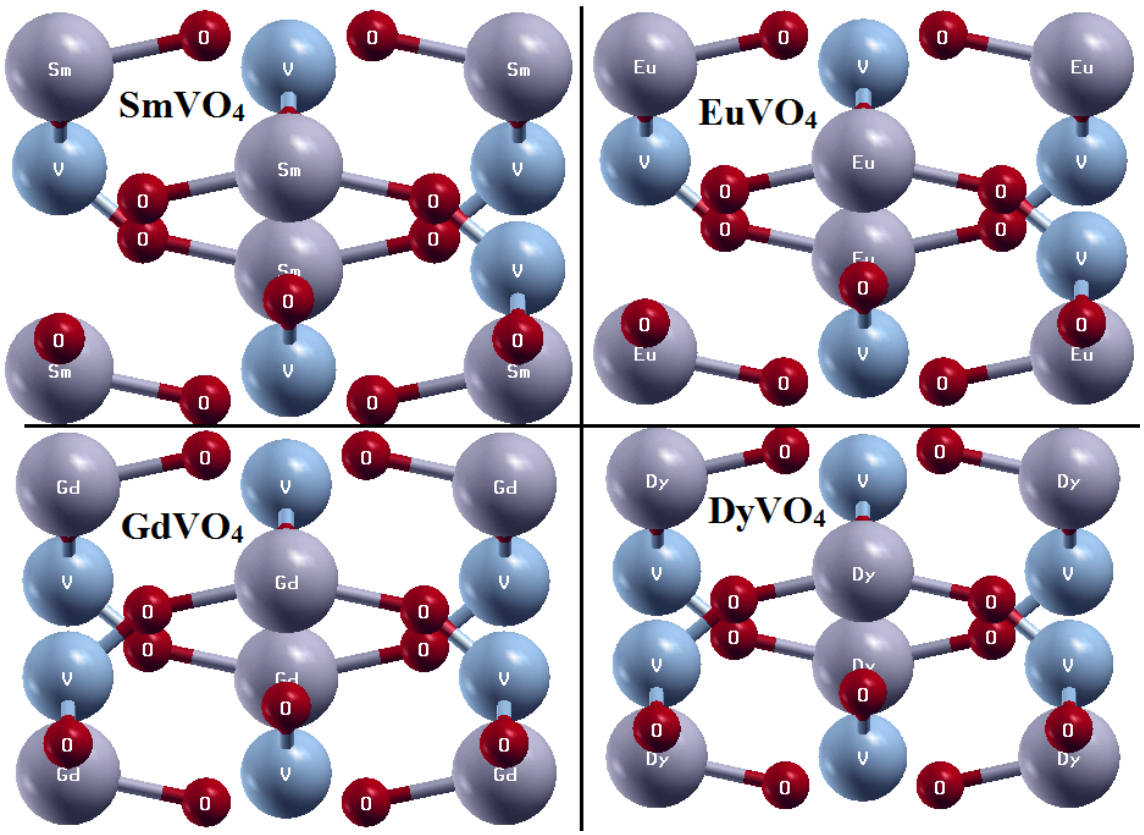

Fig. 1

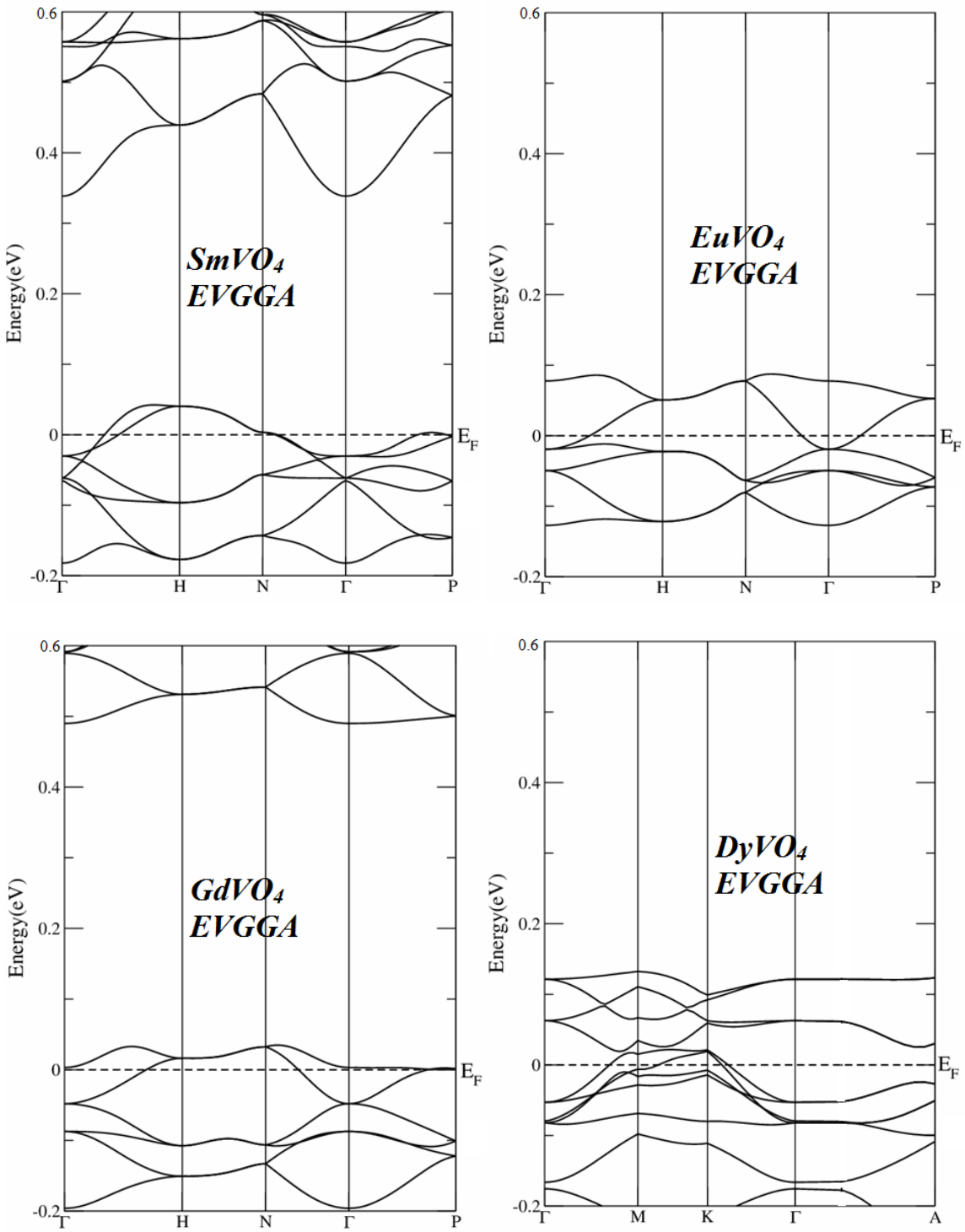
SmVO4
EVGGA
EuVO4
EVGGA
GdVO4
EVGGA
DyVO4
EVGGA
Energy(eV)
0.6
0.4
0.2
0
-0.2
E_F
Γ
H
N
P
M
K
A

Fig. 2

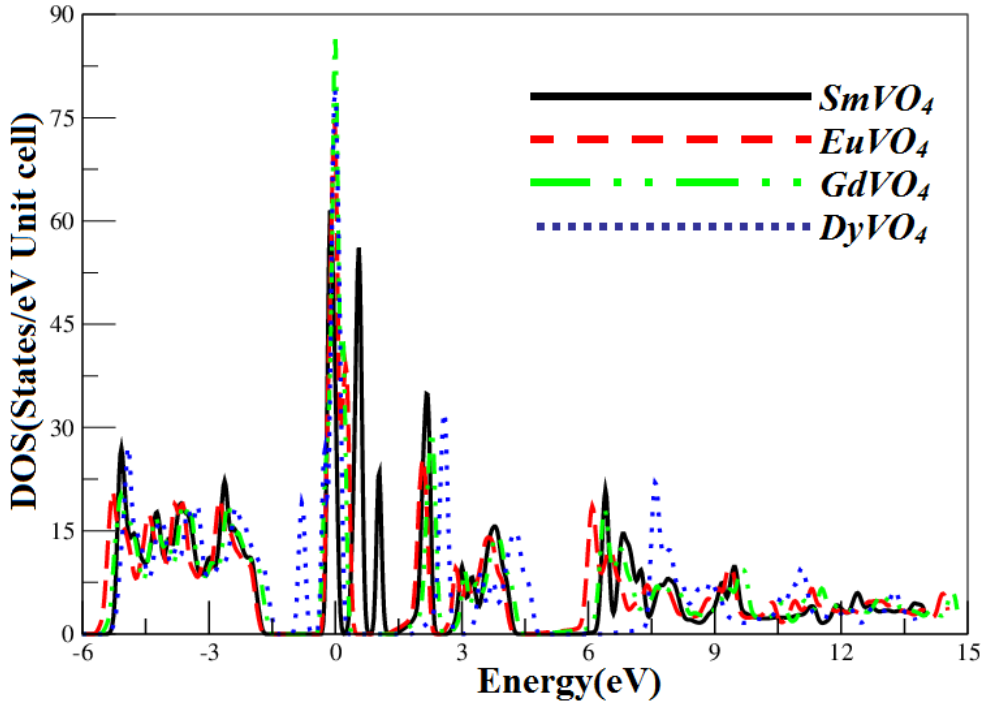
DOS(States/eV Unit cell)
Energy(eV)
SmVO4
EuVO4
GdVO4
DyVO4

Fig. 3

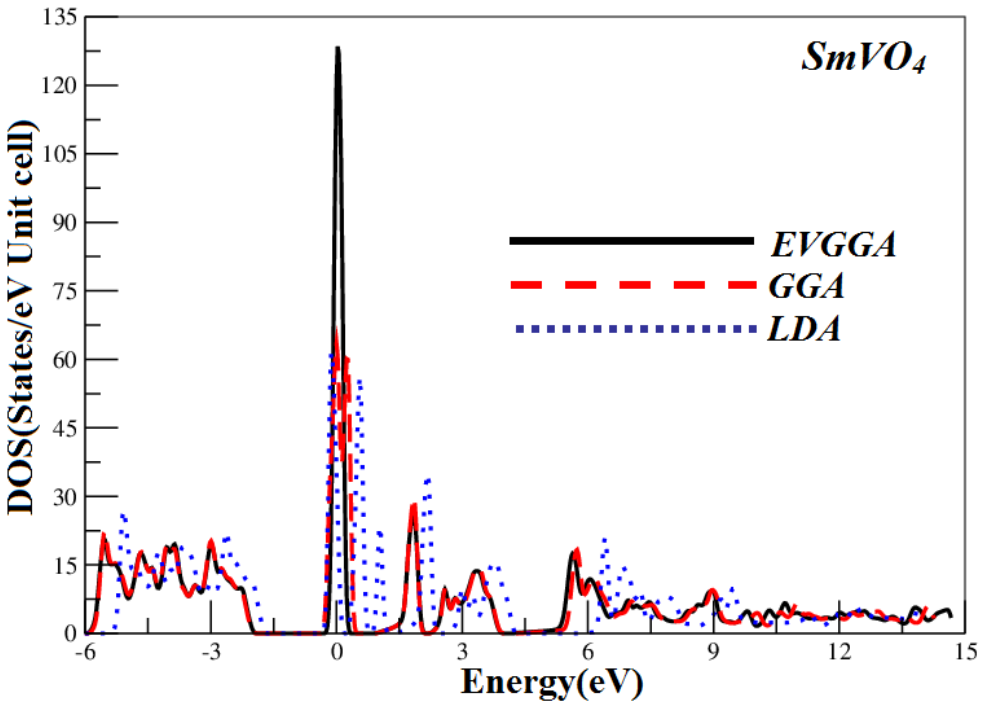
DOS(States/eV Unit cell)
Energy(eV)
SmVO4
EVGGA
GGA
LDA

(a)

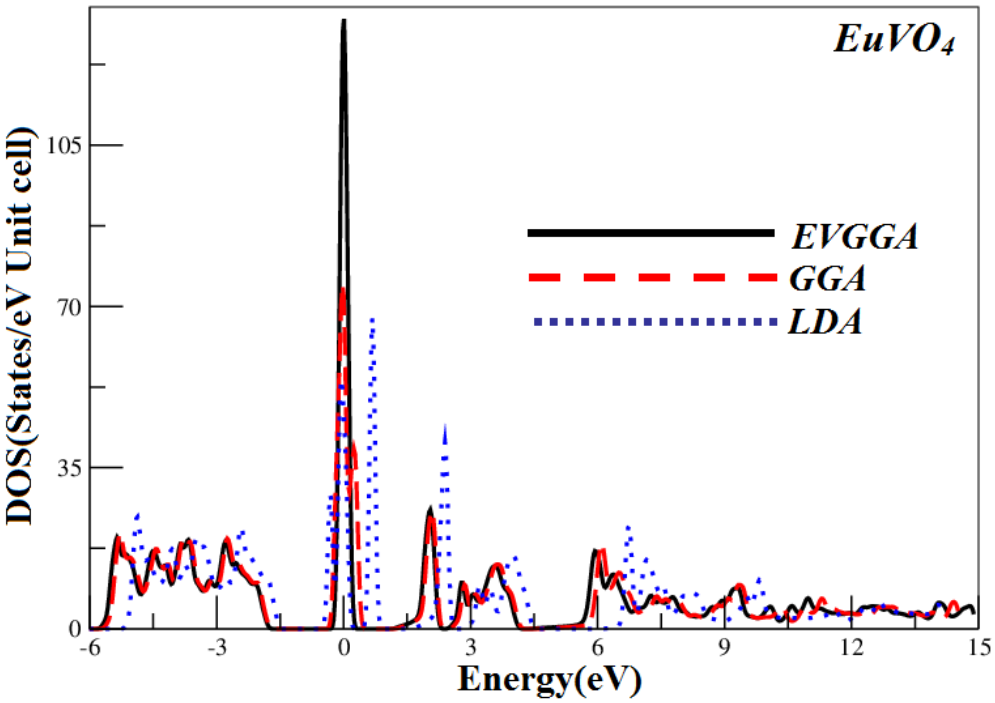
EuVO4
EVGGA
GGA
LDA
DOS(States/eV Unit cell)
Energy(eV)
0
35
70
105
-6
-3
0
3
6
9
12
15

(b)

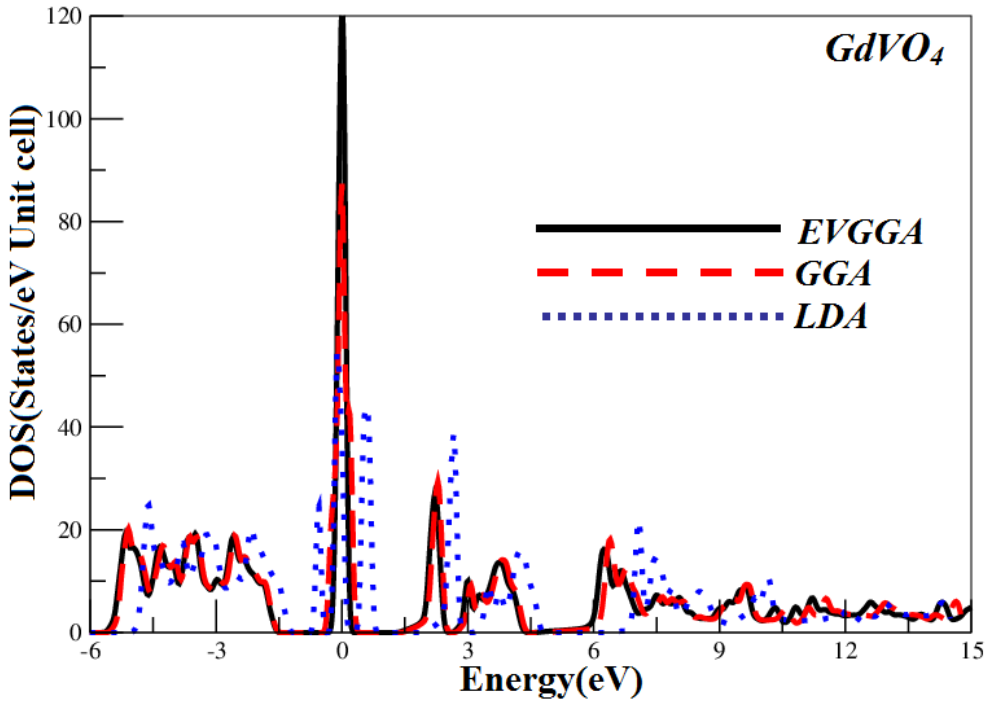
GdVO4
EVGGA
GGA
LDA
DOS(States/eV Unit cell)
Energy(eV)
0
20
40
60
80
100
120
-6
-3
0
3
6
9
12
15

(c)

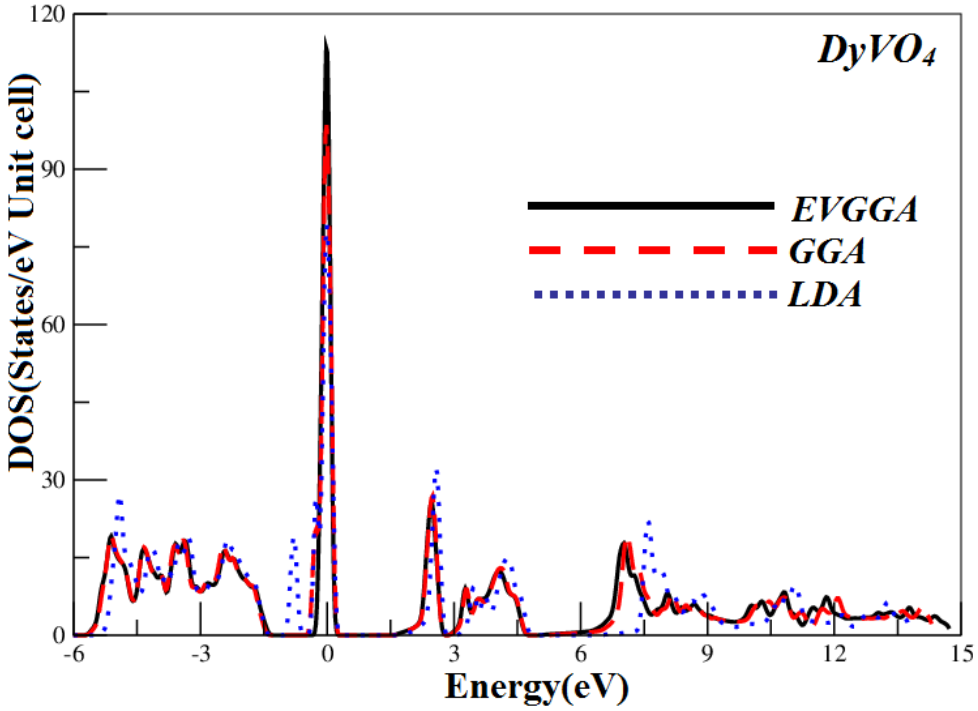
DyVO4
EVGGA
GGA
LDA
DOS(States/eV Unit cell)
Energy(eV)
120
90
60
30
0
-6
-3
0
3
6
9
12
15

(d)

Fig. 4

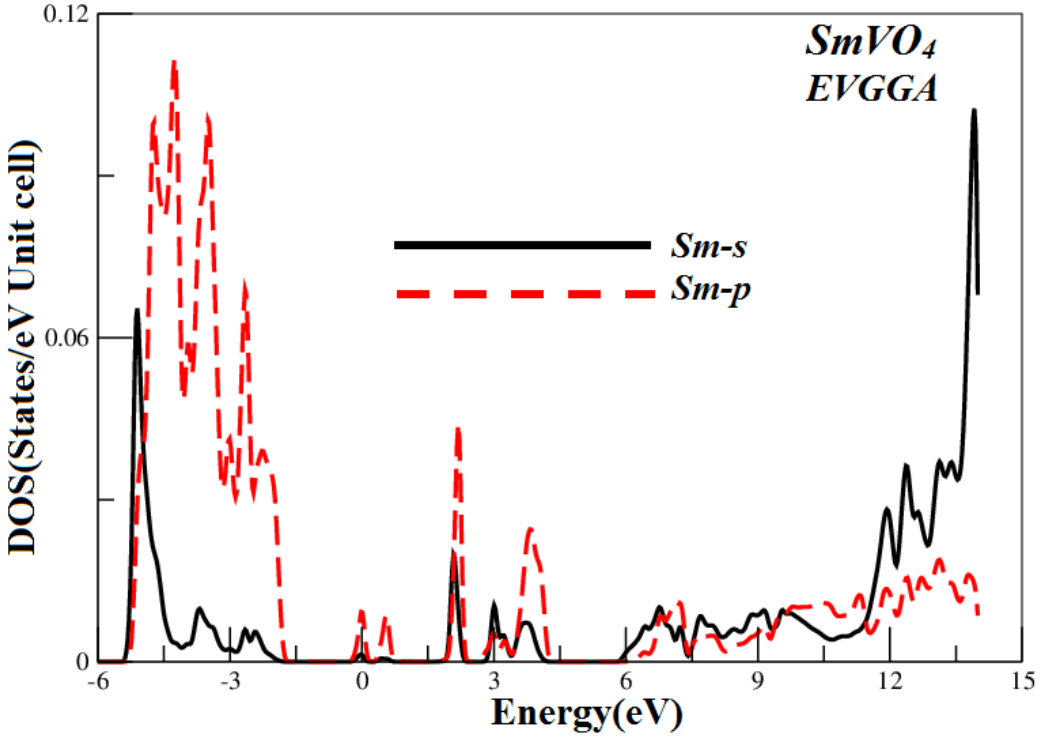
SmVO4
EVGGA
Sm-s
Sm-p
DOS(States/eV Unit cell)
Energy(eV)
0.12
0.06
0
-6
-3
0
3
6
9
12
15

(a)

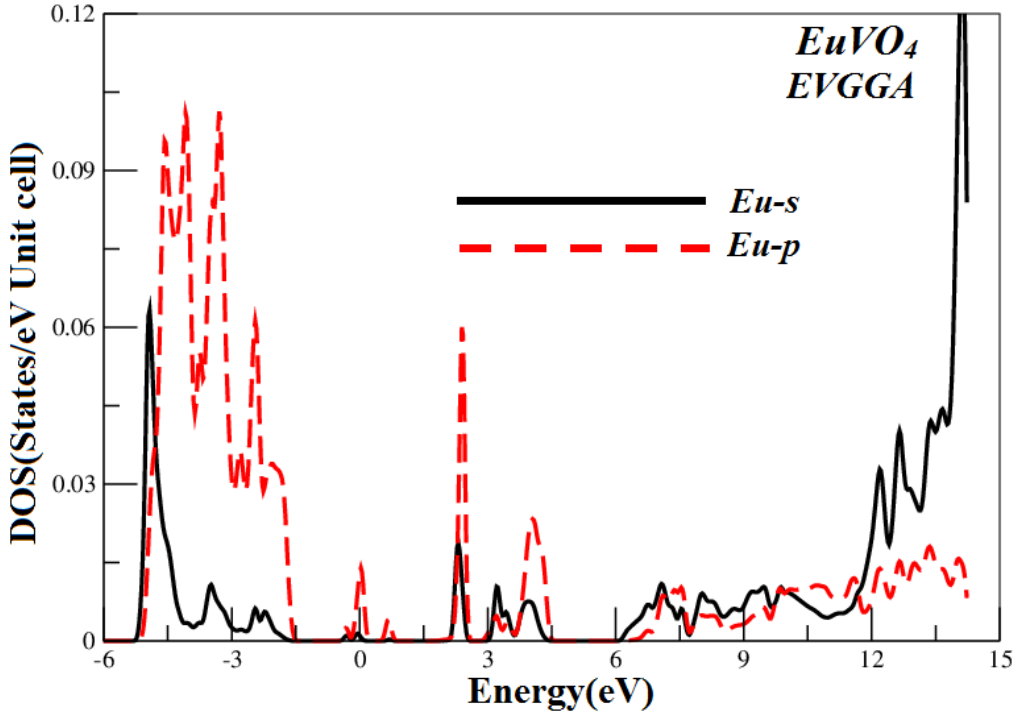
EuVO4
EVGGA
Eu-s
Eu-p
DOS(States/eV Unit cell)
Energy(eV)
0.12
0.09
0.06
0.03
0
-6
-3
0
3
6
9
12
15

(b)

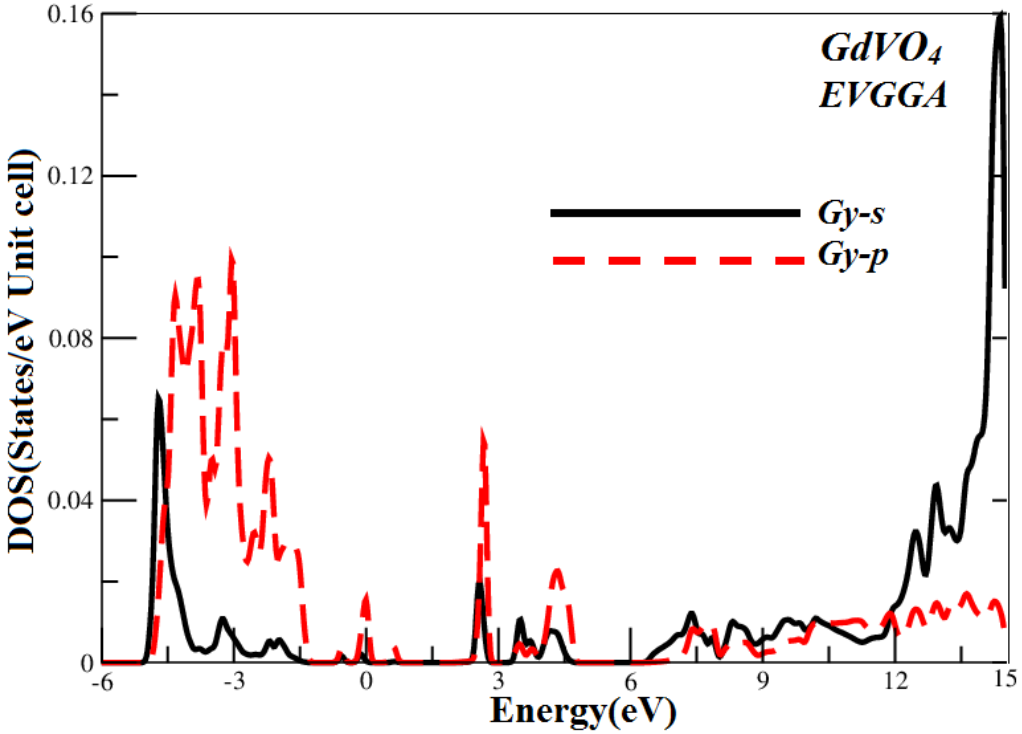
GdVO4
EVGGA
Gy-s
Gy-p
DOS(States/eV Unit cell)
Energy(eV)
0.16
0.12
0.08
0.04
0
-6
-3
0
3
6
9
12
15

(c)

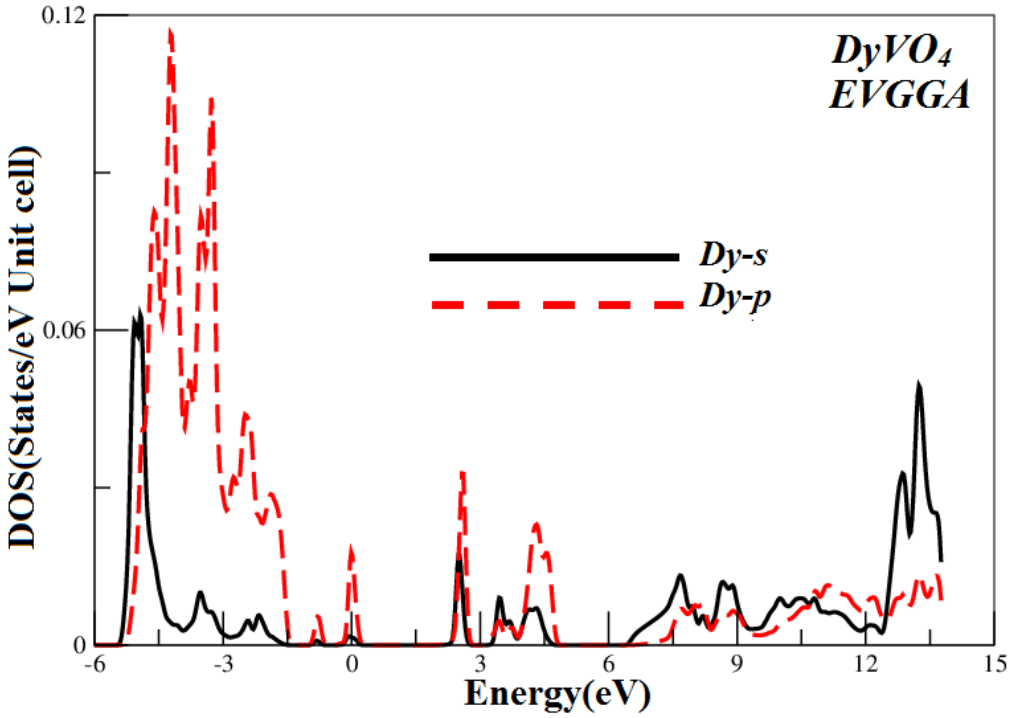
DyVO4
EVGGA
Dy-s
Dy-p
DOS(States/eV Unit cell)
Energy(eV)
0.12
0.06
0
-6
-3
0
3
6
9
12
15

(d)

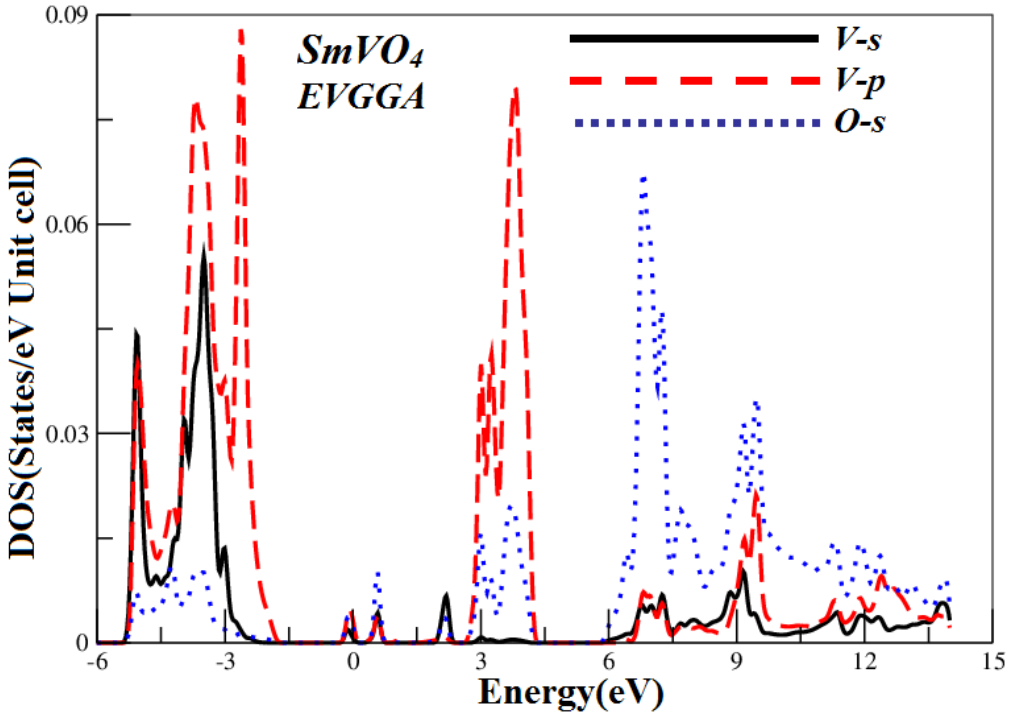
SmVO4
EVGGA
V-s
V-p
O-s
DOS(States/eV Unit cell)
Energy(eV)
0.09
0.06
0.03
0
-6
-3
0
3
6
9
12
15

(e)

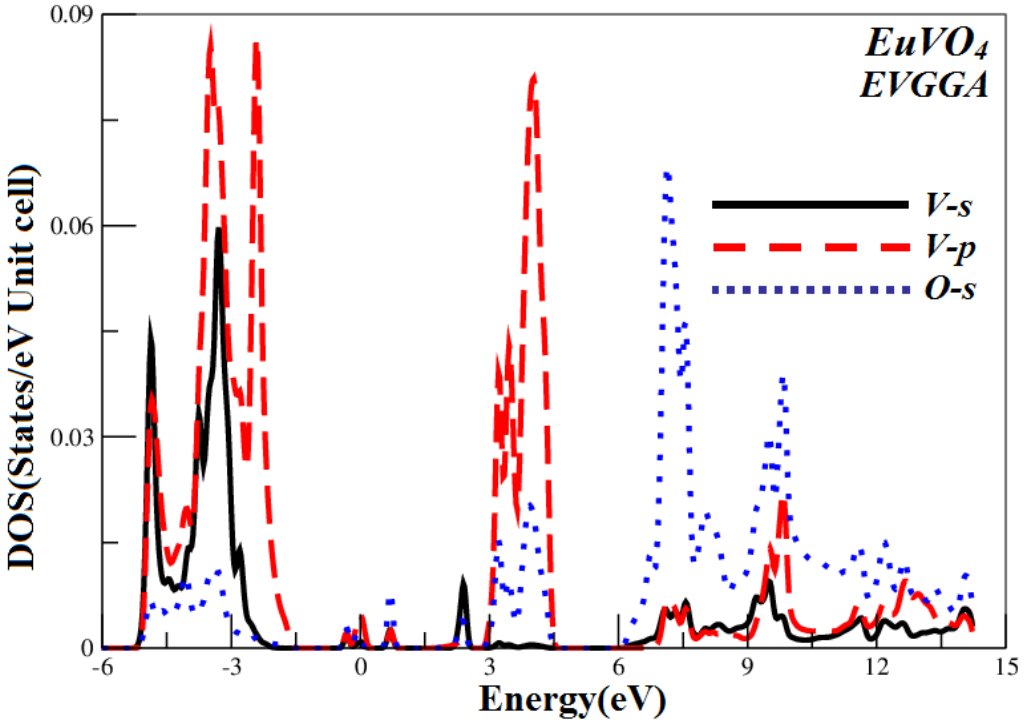
EuVO4
EVGGA
V-s
V-p
O-s
DOS(States/eV Unit cell)
Energy(eV)
0.09
0.06
0.03
0
-6
-3
0
3
6
9
12
15

(f)

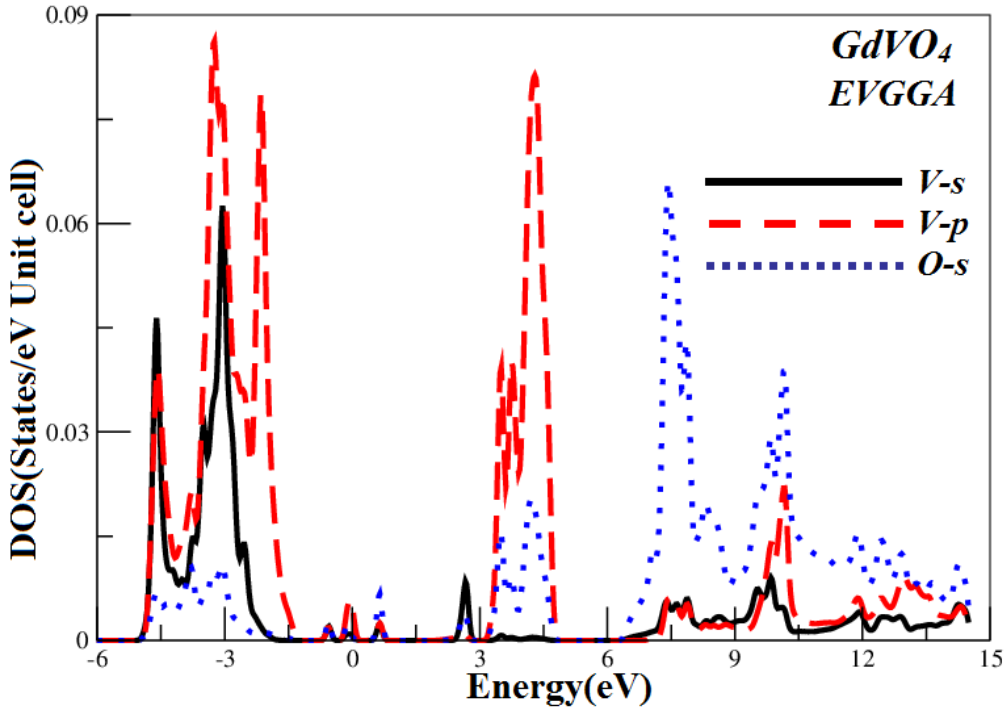
GdVO4
EVGGA
V-s
V-p
O-s
DOS(States/eV Unit cell)
Energy(eV)
0.09
0.06
0.03
0
-6
-3
0
3
6
9
12
15

(g)

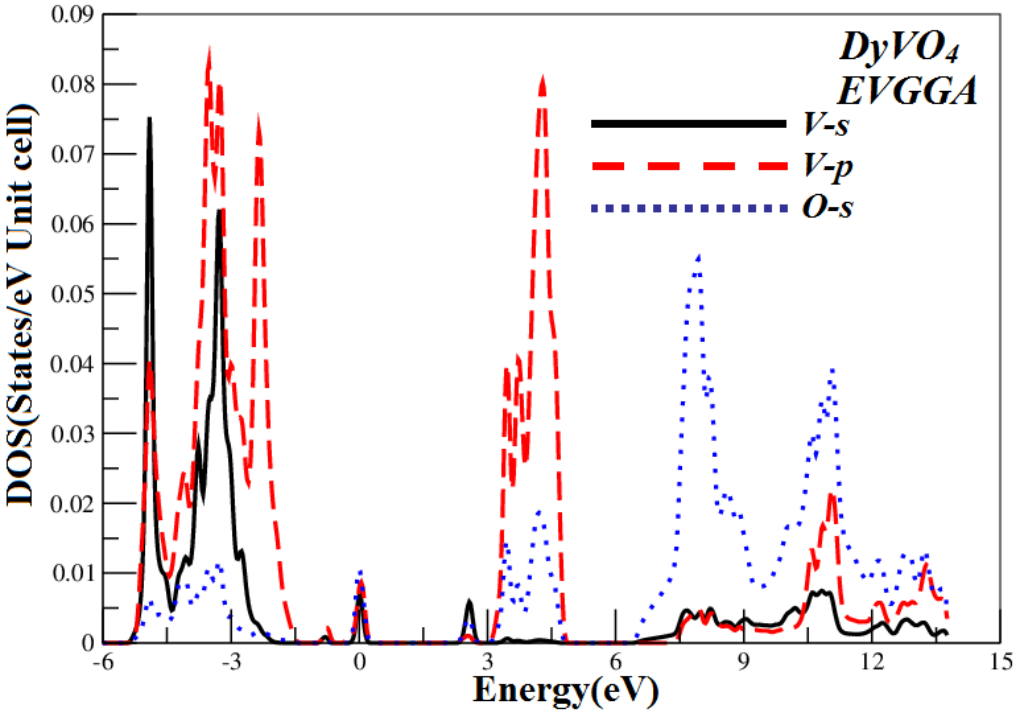
DyVO4
EVGGA
V-s
V-p
O-s
DOS(States/eV Unit cell)
Energy(eV)
0.09
0.08
0.07
0.06
0.05
0.04
0.03
0.02
0.01
0
-6
-3
0
3
6
9
12
15

(h)

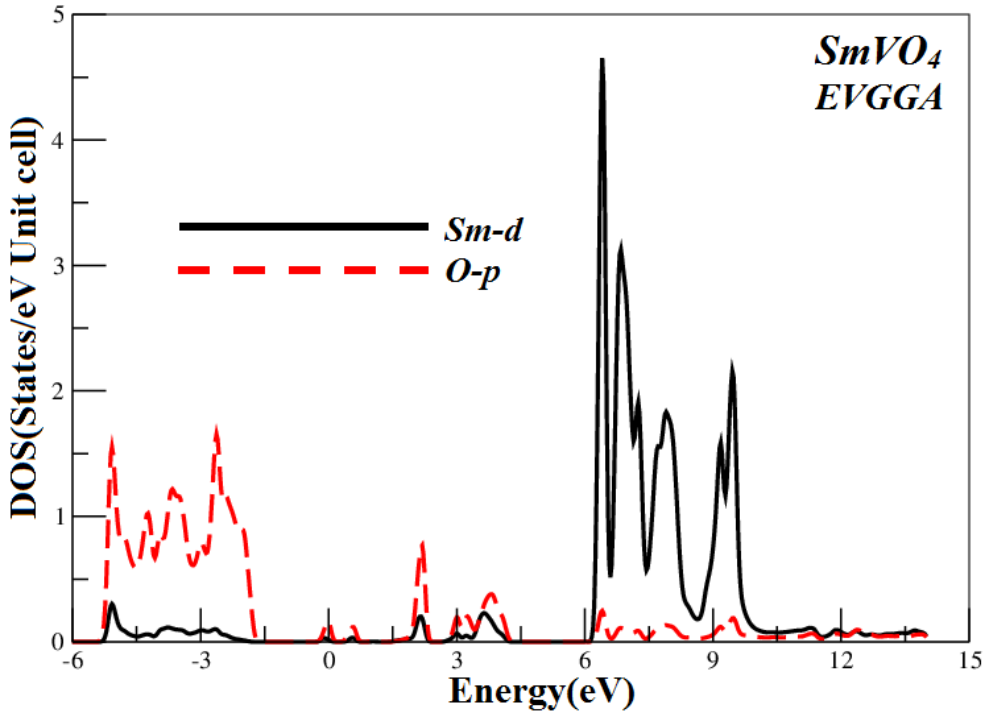
SmVO4
EVGGA
Sm-d
O-p
DOS(States/eV Unit cell)
Energy(eV)
5
4
3
2
1
0
-6
-3
0
3
6
9
12
15

(h)

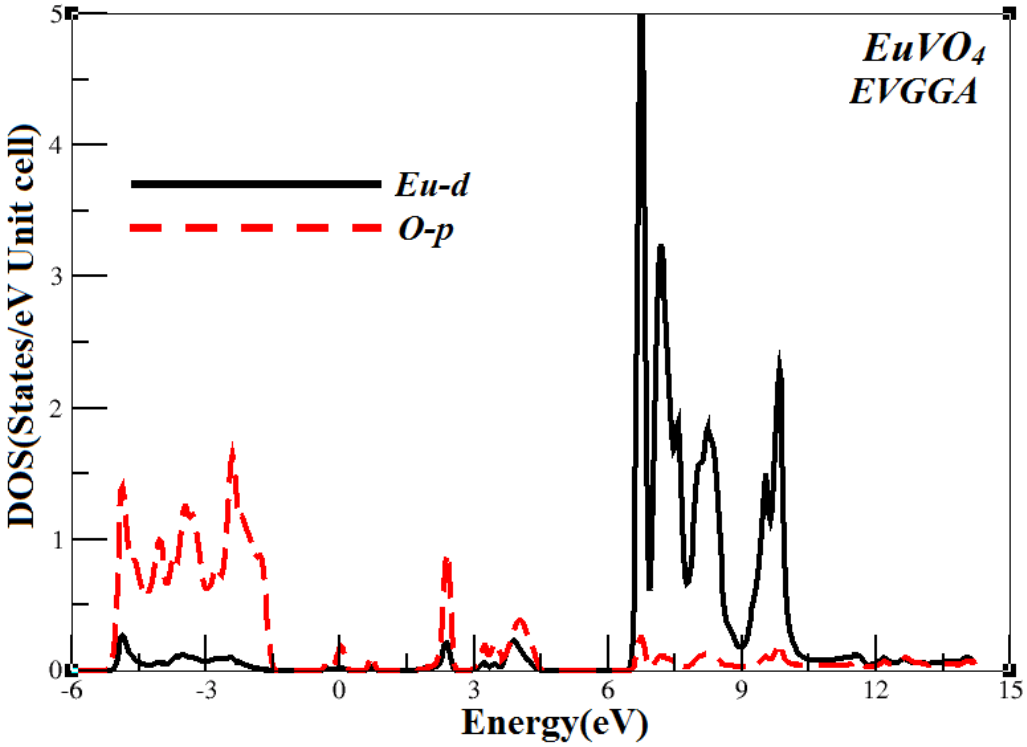
EuVO4
EVGGA
Eu-d
O-p
DOS(States/eV Unit cell)
Energy(eV)
0
1
2
3
4
5
-6
-3
0
3
6
9
12
15

(i)

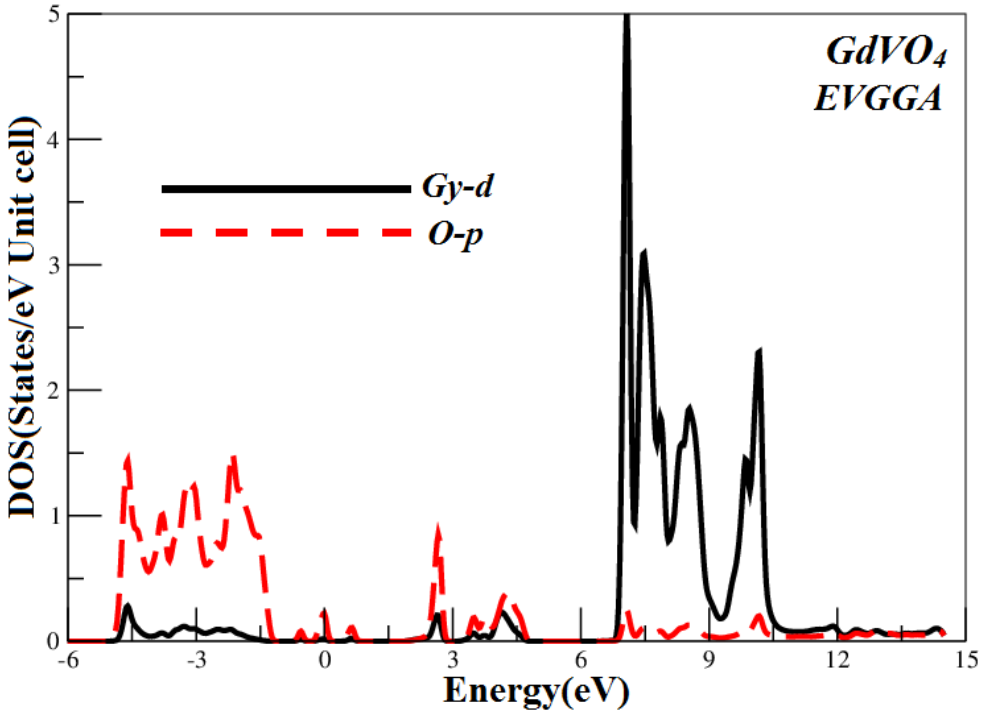
GdVO4
EVGGA
Gy-d
O-p
DOS(States/eV Unit cell)
Energy(eV)
0
1
2
3
4
5
-6
-3
0
3
6
9
12
15

(j)

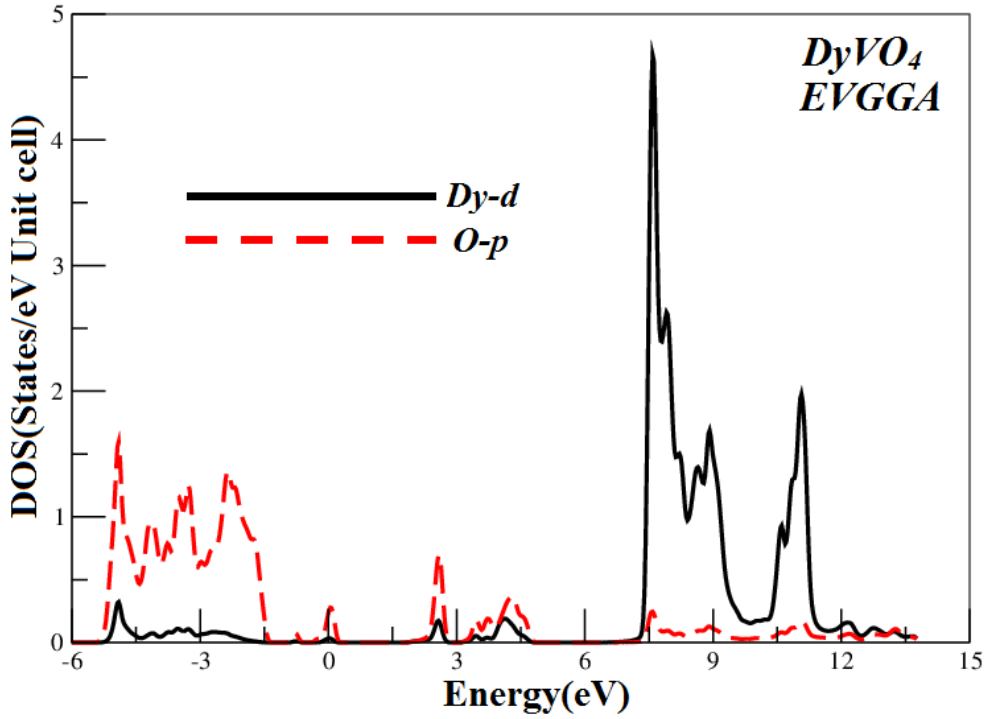
DyVO4
EVGGA
Dy-d
O-p
DOS(States/eV Unit cell)
Energy(eV)
0
1
2
3
4
5
-6
-3
0
3
6
9
12
15

(k)

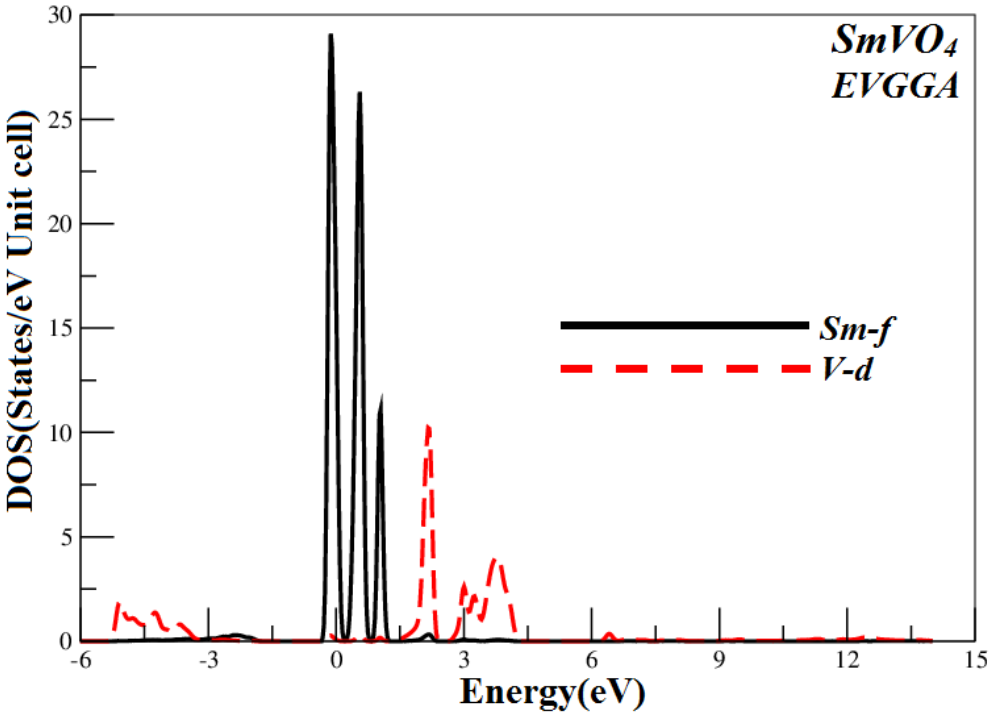
SmVO4
EVGGA
Sm-f
V-d
DOS(States/eV Unit cell)
Energy(eV)
0
5
10
15
20
25
30
-6
-3
0
3
6
9
12
15

(l)

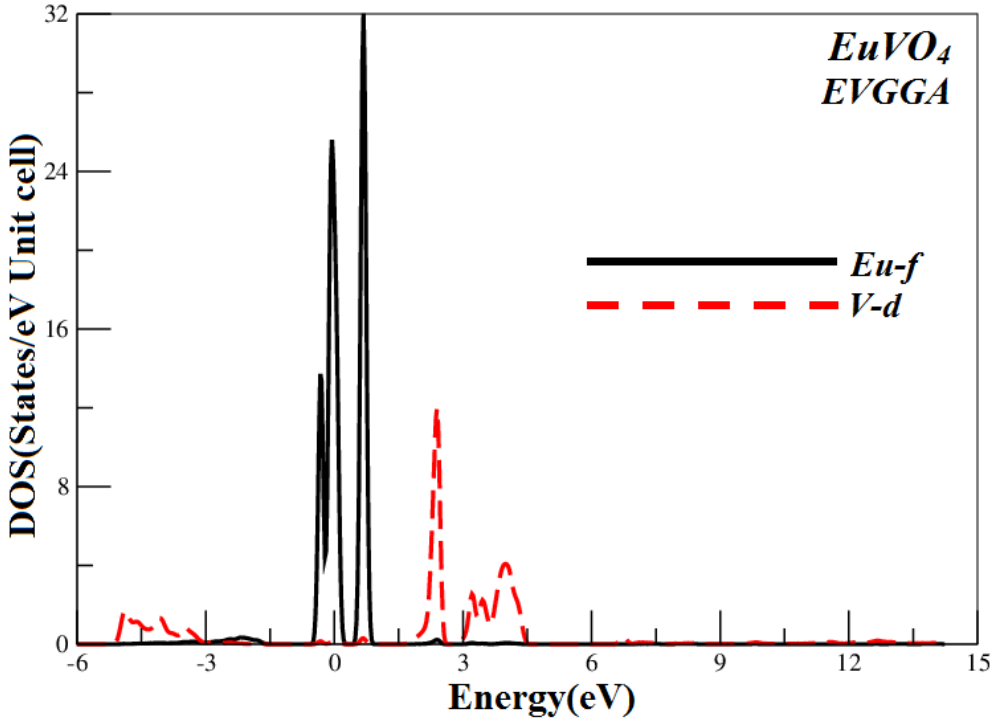
EuVO4
EVGGA
Eu-f
V-d
DOS(States/eV Unit cell)
Energy(eV)
0
8
16
24
32
-6
-3
0
3
6
9
12
15

(m)

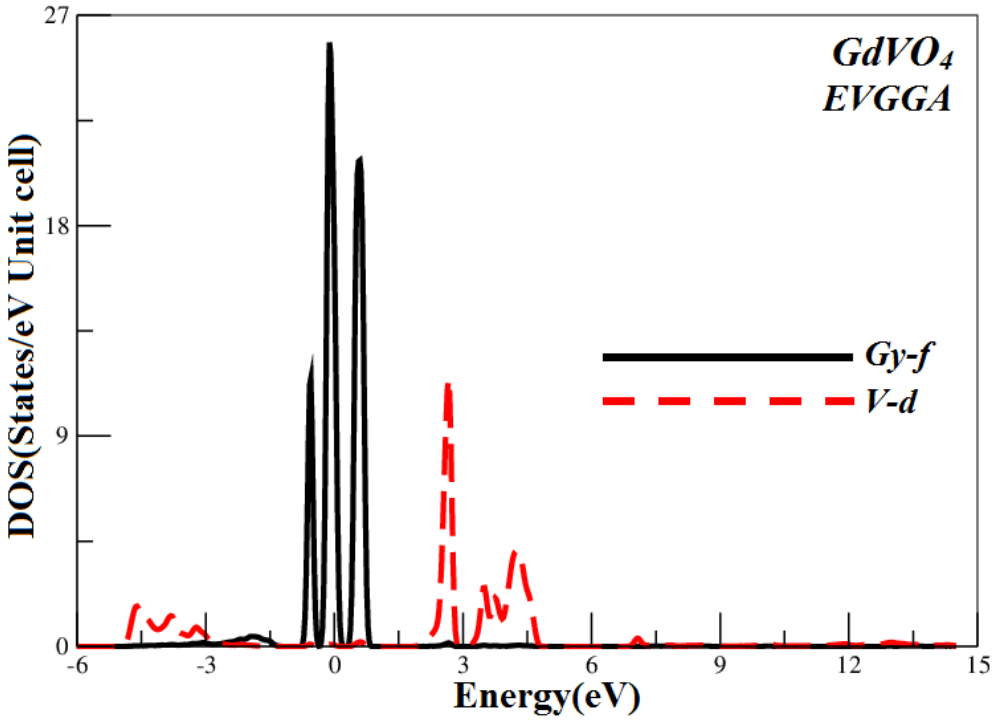
GdVO4
EVGGA
Gy-f
V-d
DOS(States/eV Unit cell)
Energy(eV)
0
9
18
27
-6
-3
0
3
6
9
12
15

(n)

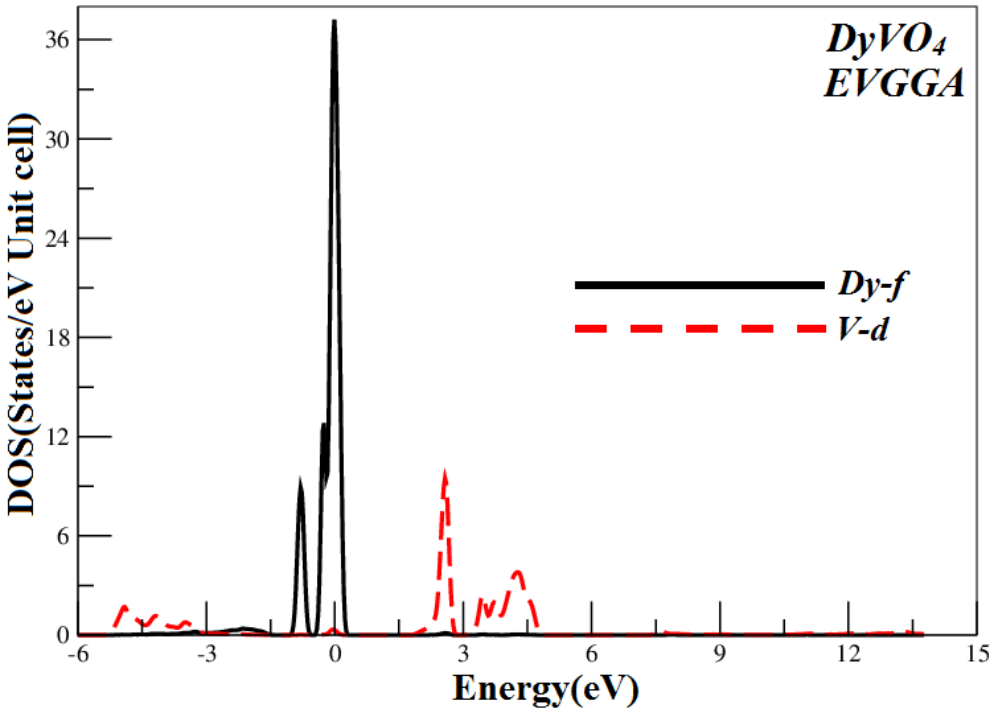
DyVO4
EVGGA
Dy-f
V-d
DOS(States/eV Unit cell)
Energy(eV)
0
6
12
18
24
30
36
-6
-3
0
3
6
9
12
15

(o)

Fig. 5

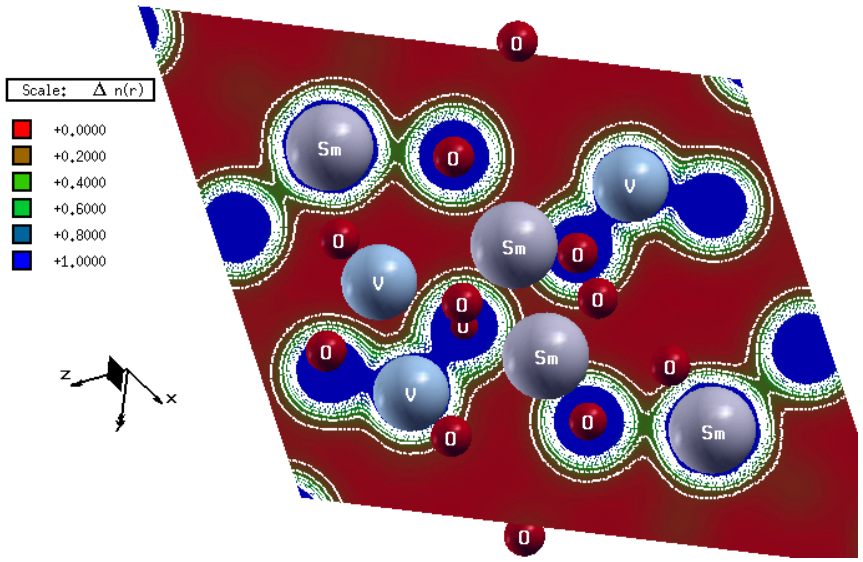
Scale: Δ n(r)
+0.0000
+0.2000
+0.4000
+0.6000
+0.8000
+1.0000
Sm
V
O
z
x

(a)

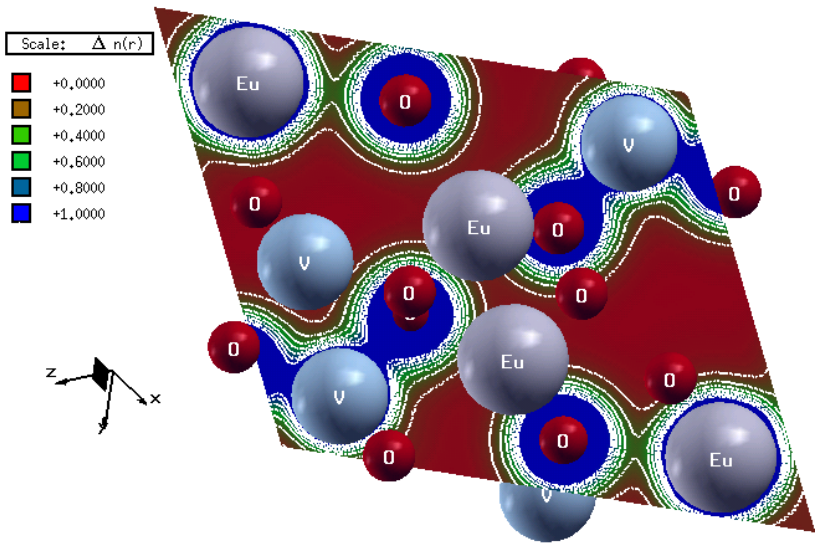
Scale: Δ n(r)
+0.0000
+0.2000
+0.4000
+0.6000
+0.8000
+1.0000
Eu
V
O
z
x

(b)

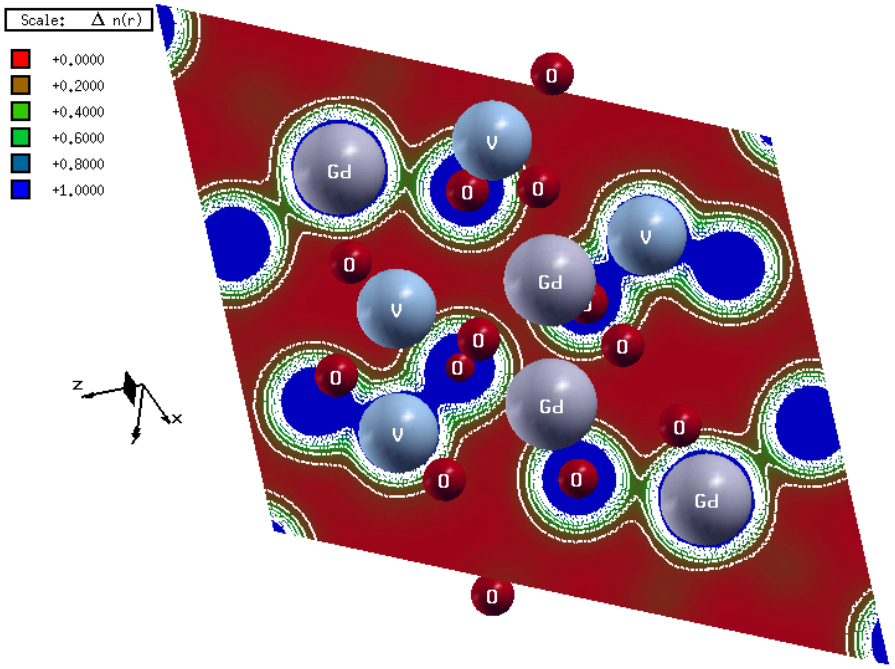
Scale: Δ n(r)
+0.0000
+0.2000
+0.4000
+0.6000
+0.8000
+1.0000
Gd
V
O
z
x

(c)

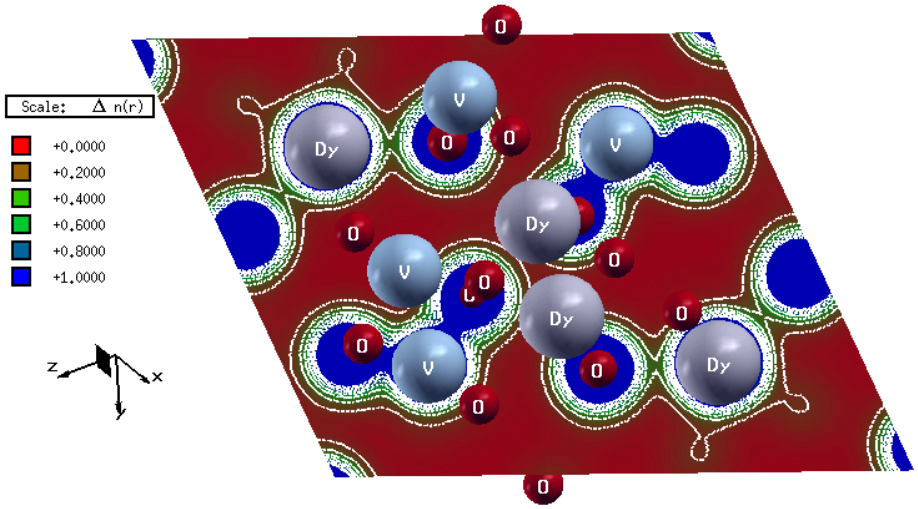

(d)

Fig. 6

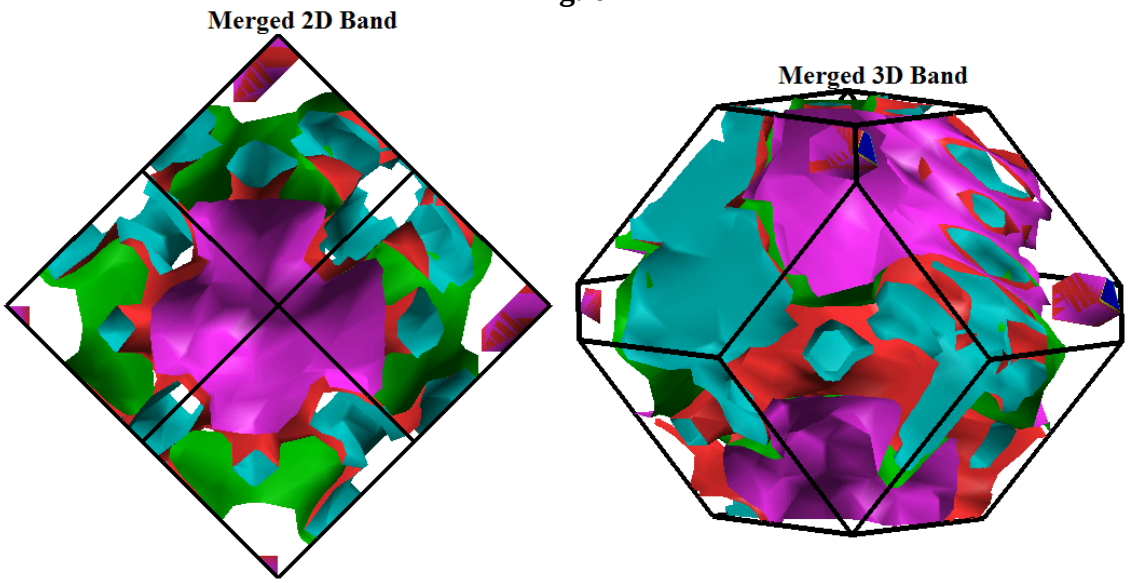

(a)

Fermi surface for $SmVO_4$

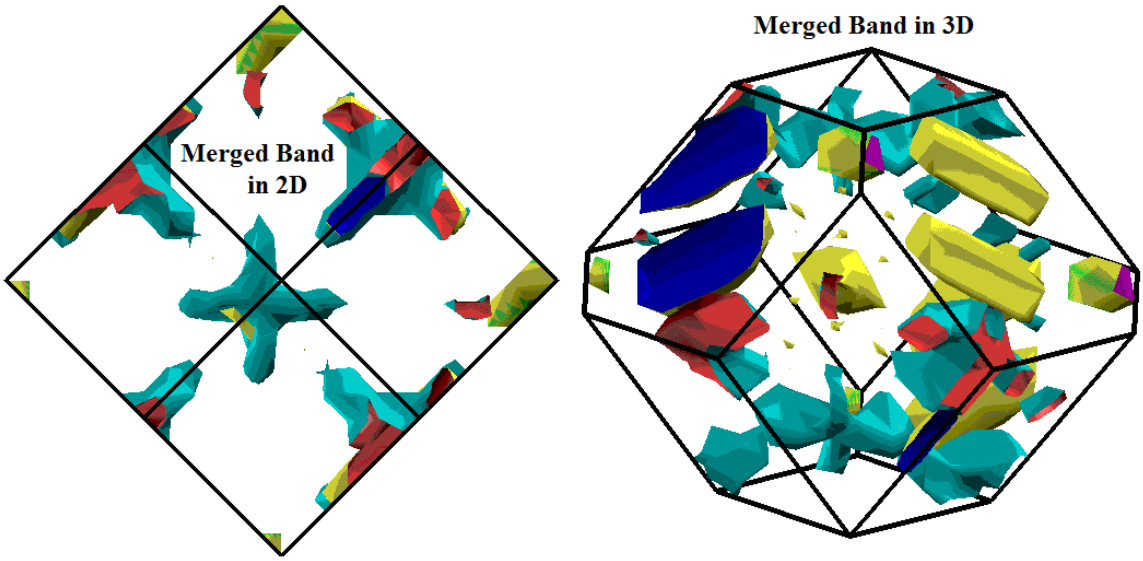

(b)

Fermi surface for $EuVO_4$

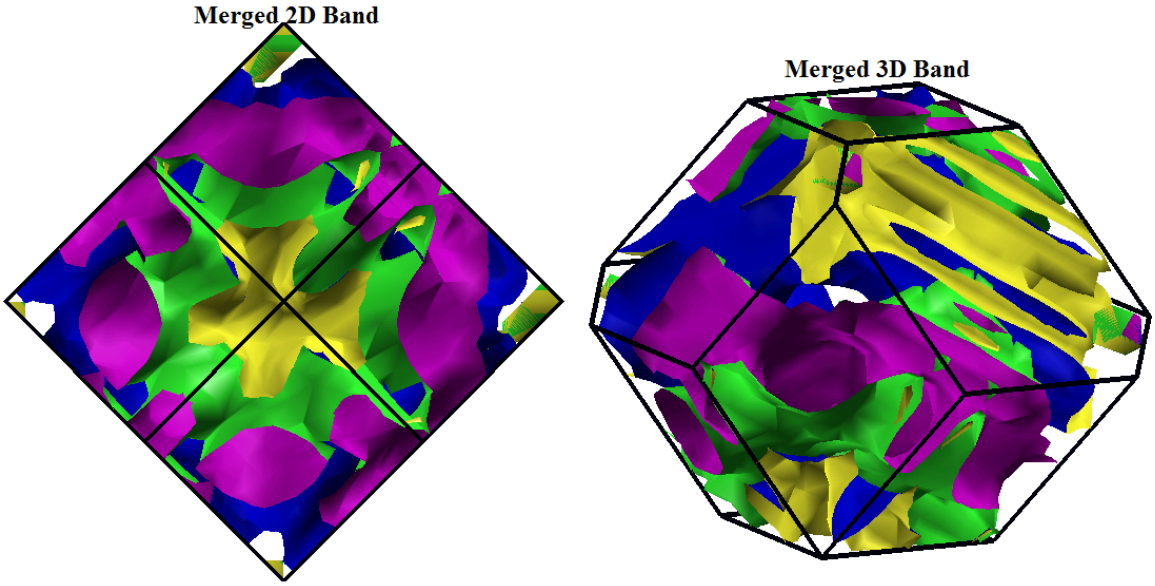

(c)

Fermi surface for $GyVO_4$

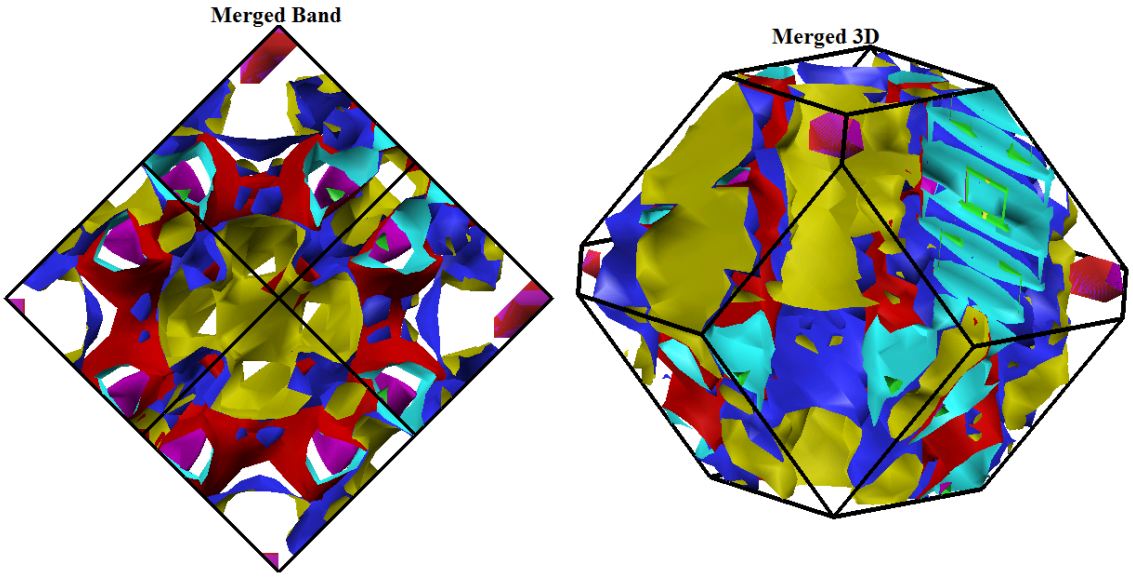

(d)

Fermi surface for $DyVO_4$
Fig. 7

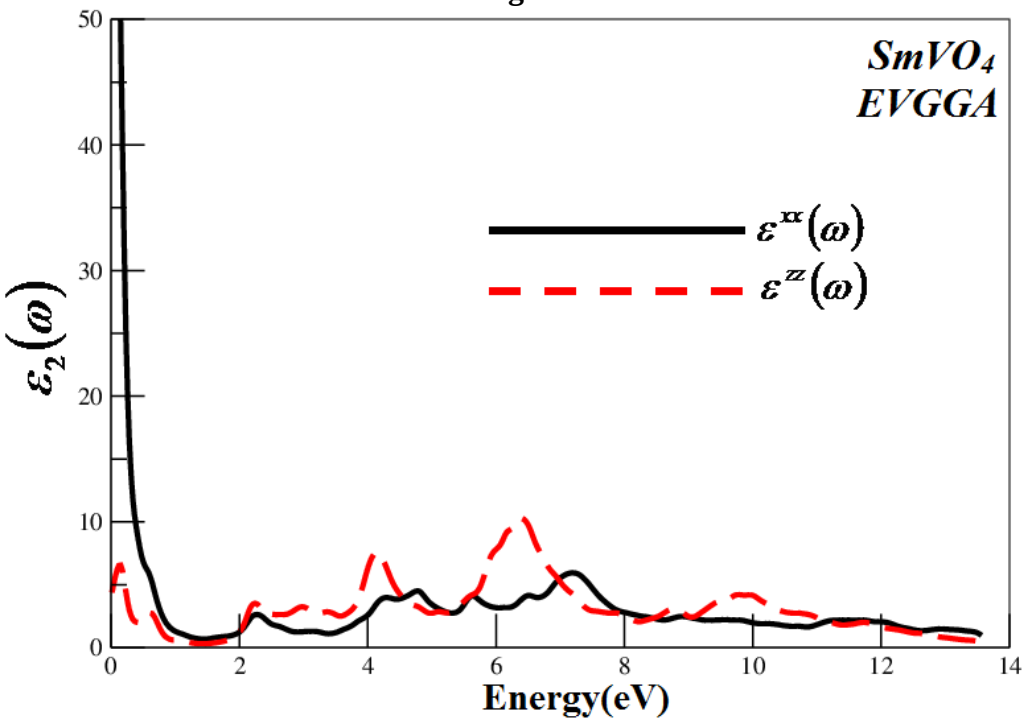

(a)

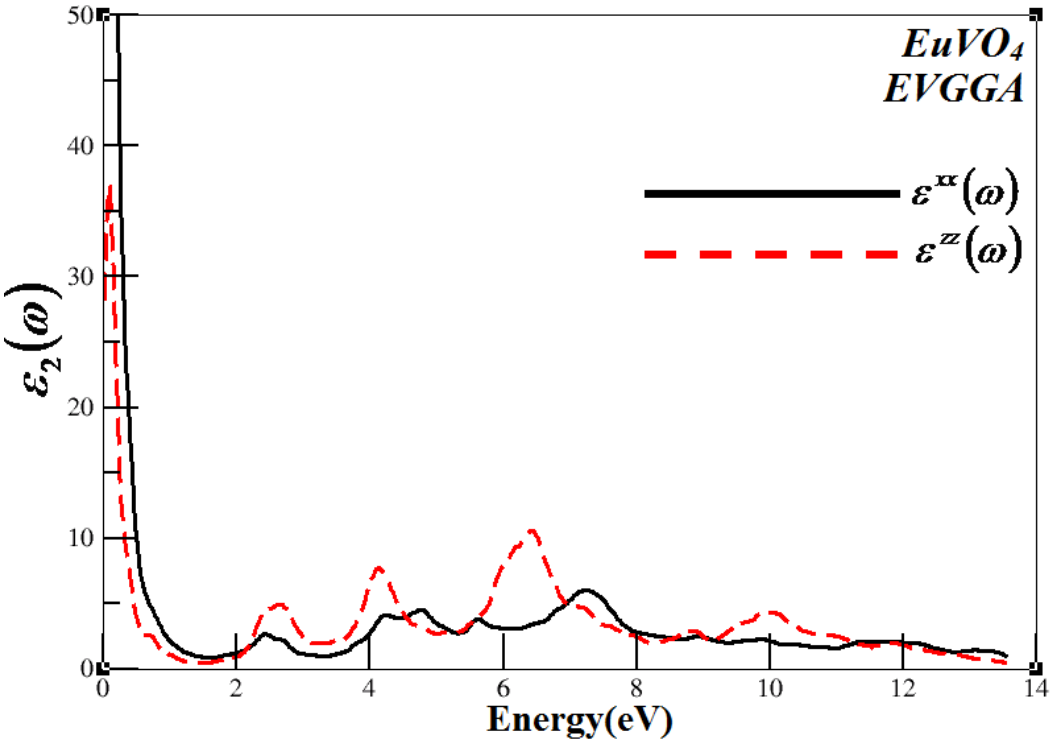
EuVO4
EVGGA
ε^xx(ω)
ε^zz(ω)
ε2(ω)
Energy(eV)
0
10
20
30
40
50
0
2
4
6
8
10
12
14

(b)

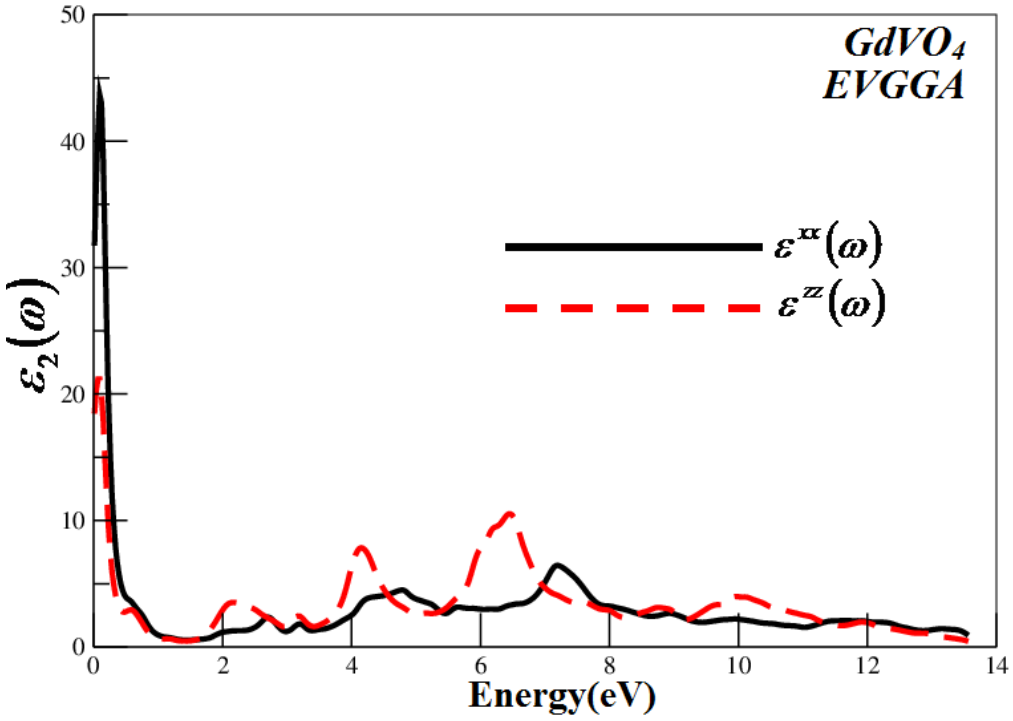
GdVO4
EVGGA
ε^xx(ω)
ε^zz(ω)
ε2(ω)
Energy(eV)
0
10
20
30
40
50
0
2
4
6
8
10
12
14

(c)

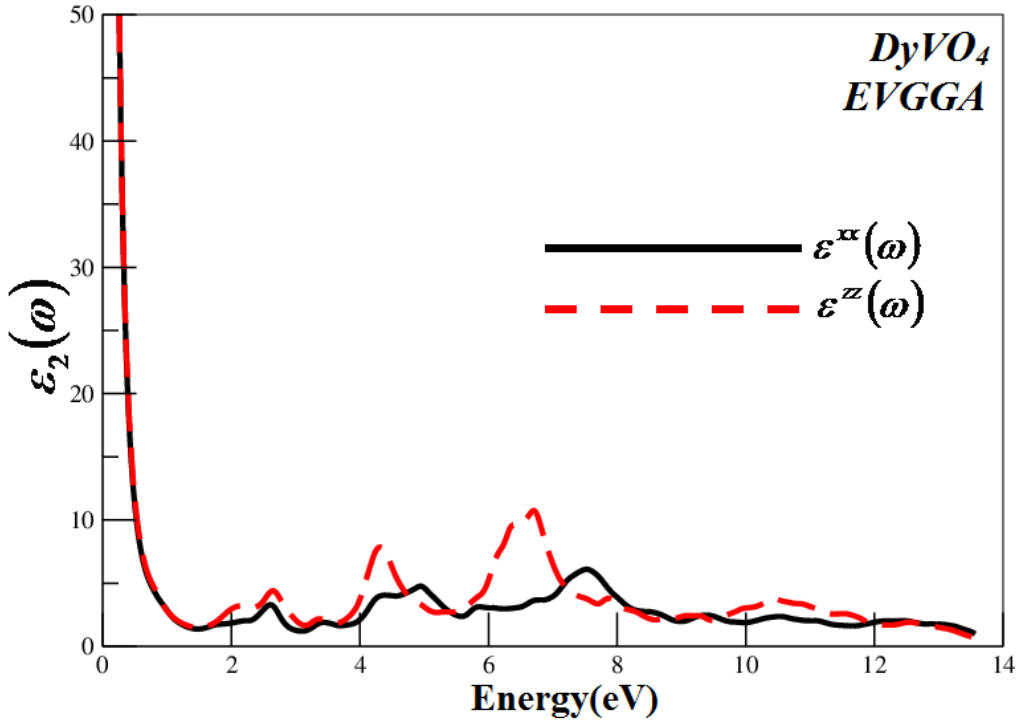
DyVO4
EVGGA
$\varepsilon^{xx}(\omega)$
$\varepsilon^{zz}(\omega)$
$\varepsilon_2(\omega)$
Energy(eV)
0
10
20
30
40
50
0
2
4
6
8
10
12
14

(d)

Fig. 8

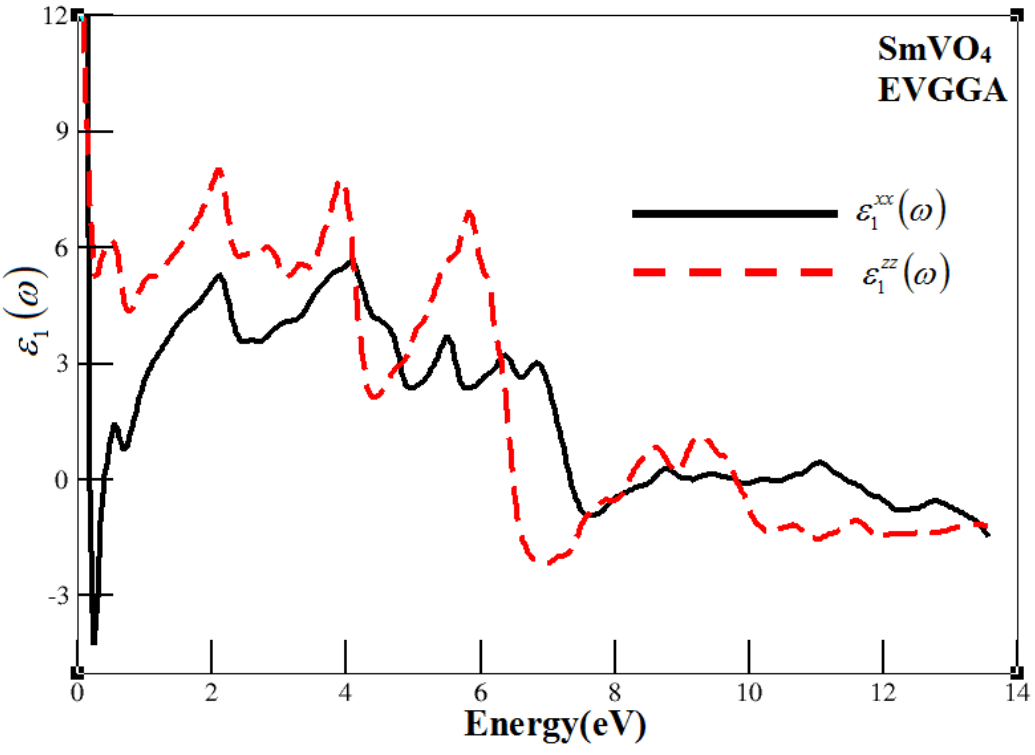
SmVO4
EVGGA
$\varepsilon_1^{xx}(\omega)$
$\varepsilon_1^{zz}(\omega)$
$\varepsilon_1(\omega)$
Energy(eV)
-3
0
3
6
9
12
0
2
4
6
8
10
12
14

(a)

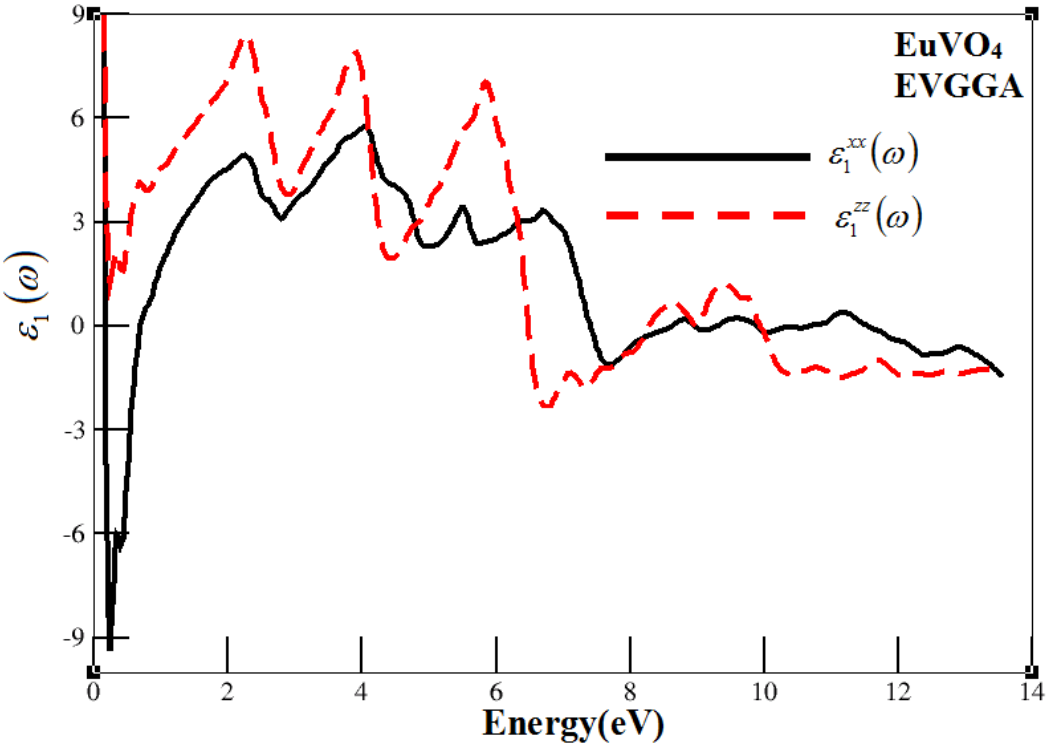
EuVO4
EVGGA
$\varepsilon_1^{xx}(\omega)$
$\varepsilon_1^{zz}(\omega)$
$\varepsilon_1(\omega)$
Energy(eV)

(b)

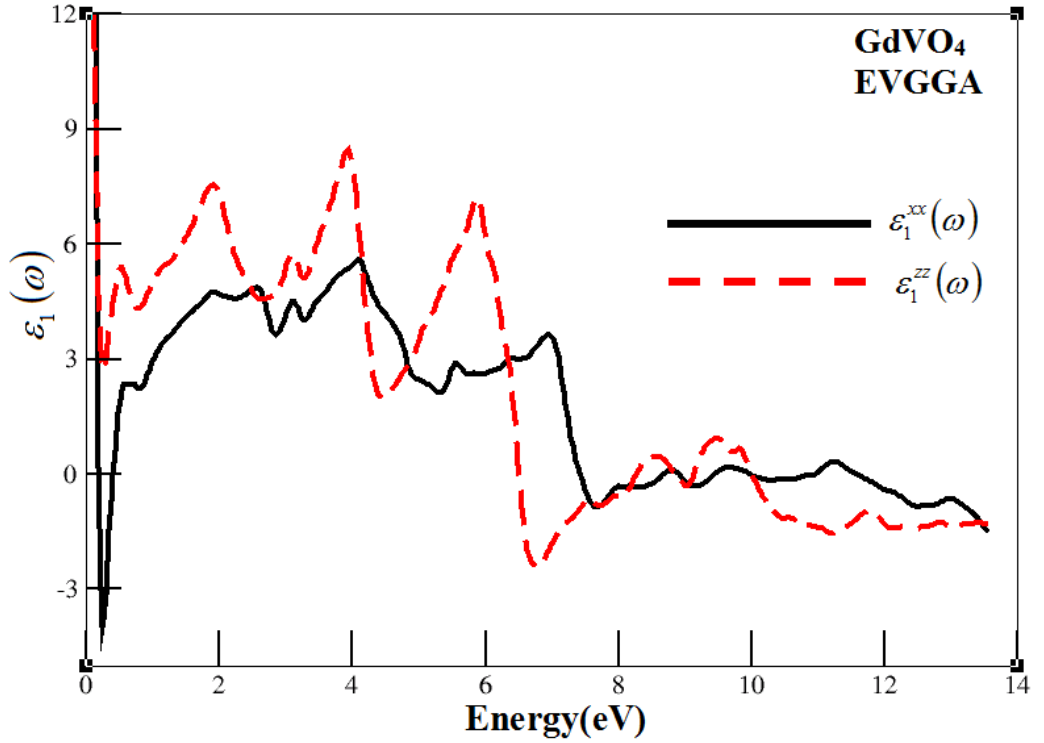
GdVO4
EVGGA
$\varepsilon_1^{xx}(\omega)$
$\varepsilon_1^{zz}(\omega)$
$\varepsilon_1(\omega)$
Energy(eV)

(c)

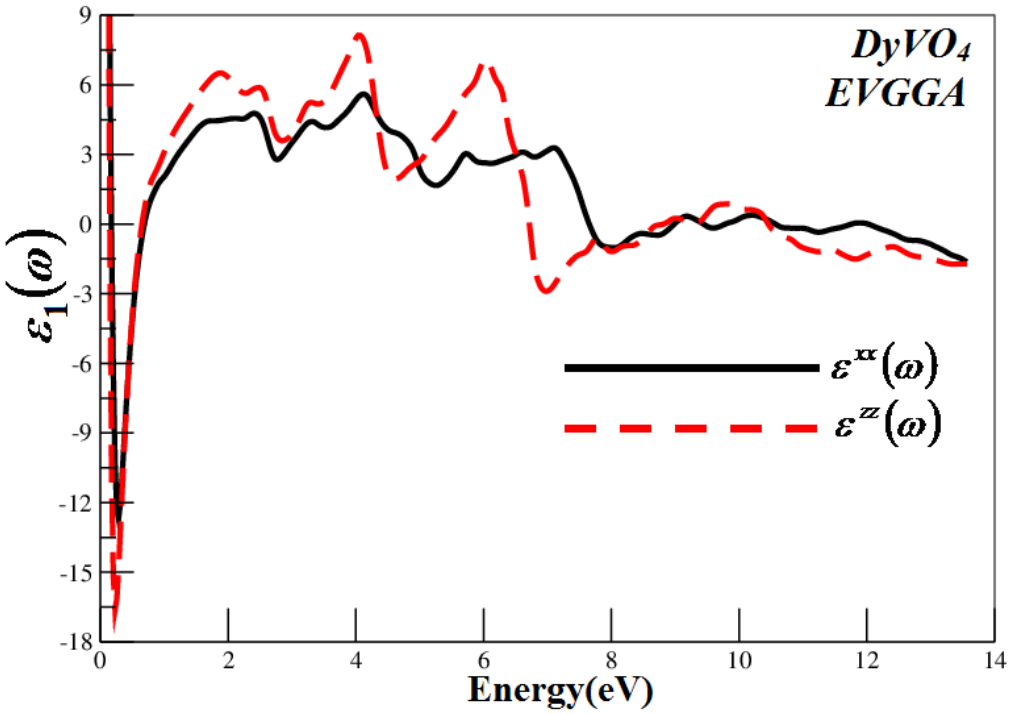
DyVO4
EVGGA
ε1(ω)
ε^xx(ω)
ε^zz(ω)
Energy(eV)
9
6
3
0
-3
-6
-9
-12
-15
-18
0
2
4
6
8
10
12
14

(d)

Fig. 9